INTiBS PAN Wrocław, 18 maja 2016 r.

Resztkowy efekt Meissnera powyżej T_c w nadprzewodnikach wysokotemperaturowych

T. Domański

Uniwersytet M. Curie-Skłodowskiej

w Lublinie

http://kft.umcs.lublin.pl/doman/lectures

INTiBS PAN Wrocław, 18 May 2016

Residual Meissner effect above T_c in high-temperature superconductors

T. Domański

M. Curie-Skłodowska University, Lublin, Poland

http://kft.umcs.lublin.pl/doman/lectures

Torque magnetometry

evidence for diamagnetism above T_c

Torque magnetometry evidence for diamagnetism above T_c

A few details:

Used samples:

$La_{2-x}Sr_xCuO_4$
$Bi_2Sr_{2-y}La_yCuO_6$
$Bi_2Sr_2Ca_yCu_2O_{8+\delta}$

Methodology:

Torque magnetisation was measured using the samples glued to the tip of a thin cantilever with $\vec{H}$ applied at a tilt angle $\theta = 10^0 - 15^0$ to the crystal c axis.

Who/where/when:

L. Li, ... and N.P. Ong, Phys. Rev. B **81**, 054510 (2010).
Princeton + Beijing + Tokyo + Ibaraki + Brookhaven

Torque magnetometry | **evidence for diamagnetism above T_c**

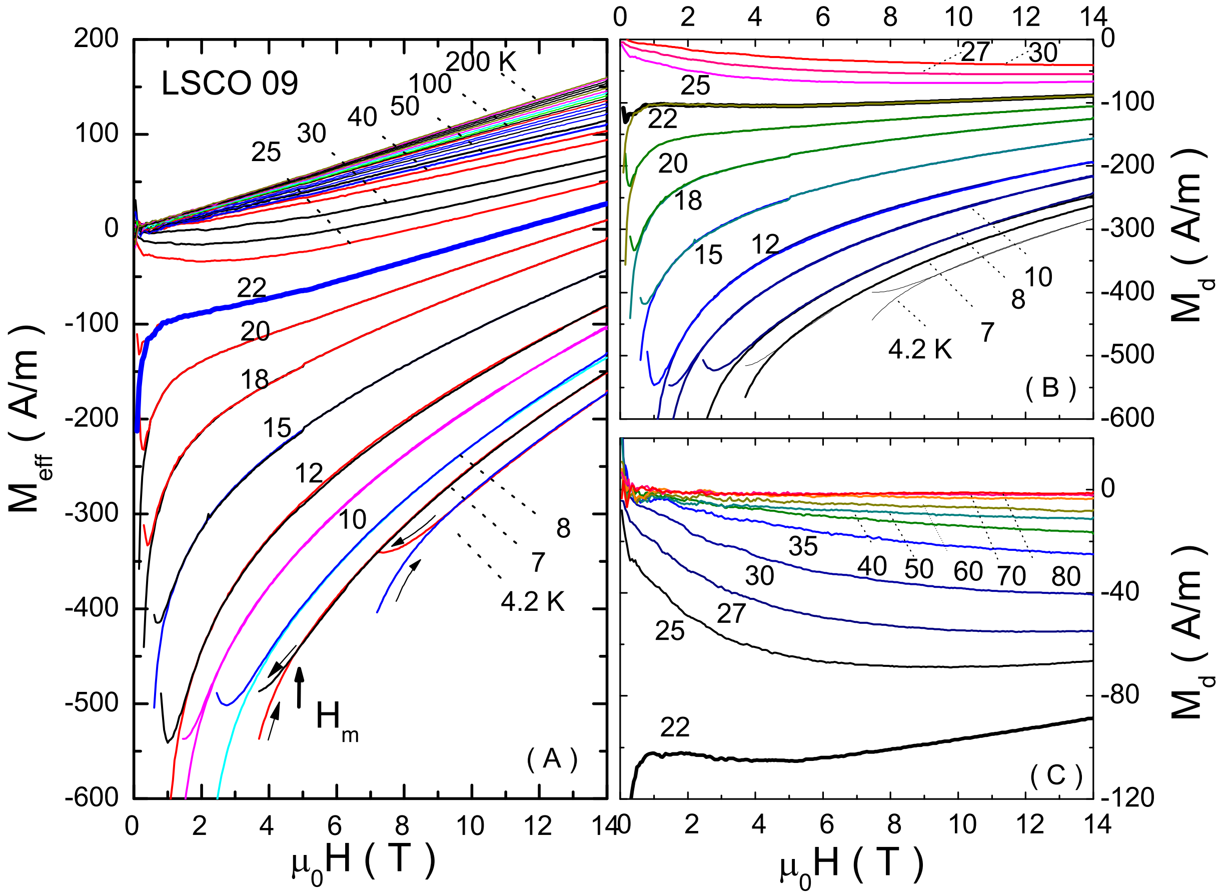

$$M_d(H) = M_{eff} - M_p$$

where

$$M_p = (A + BT)\, H$$

$$T_c = 24K$$

Magnetisation of $La_{2-x}Sr_xCuO_4$ sample with $x = 0.09$ content of Sr.

Torque magnetometry

evidence for diamagnetism above T_c

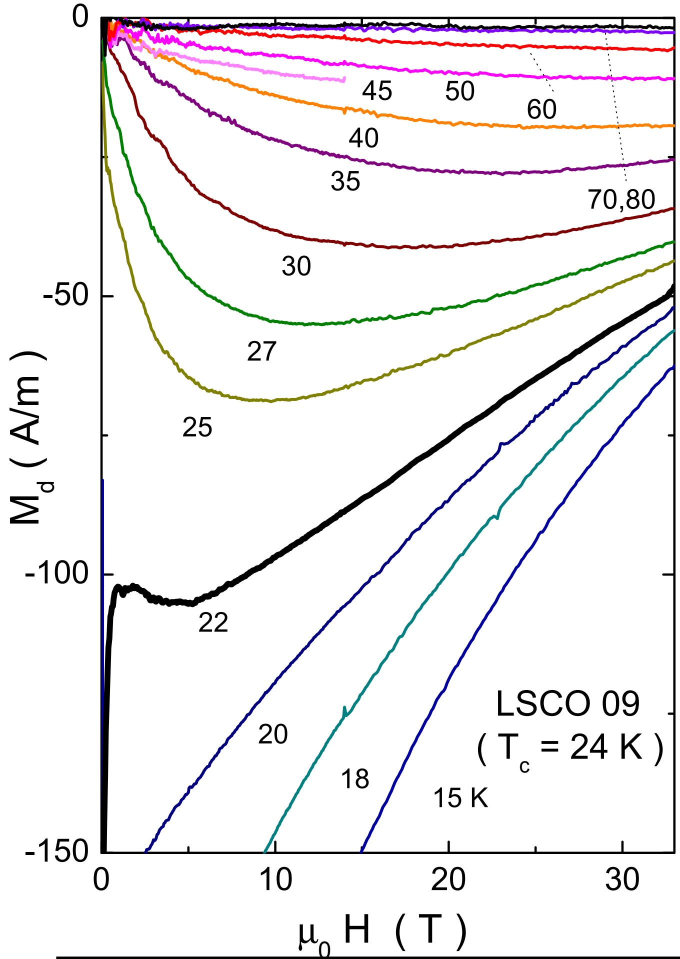

$M_d(H)$ **measured in the strong magnetic field up to 33 T.**

$$T_c = 24K$$

Magnetisation of La$_{2-x}$Sr$_x$CuO$_4$ sample with $x = 0.09$ content of Sr.

Torque magnetometry

evidence for diamagnetism above T_c

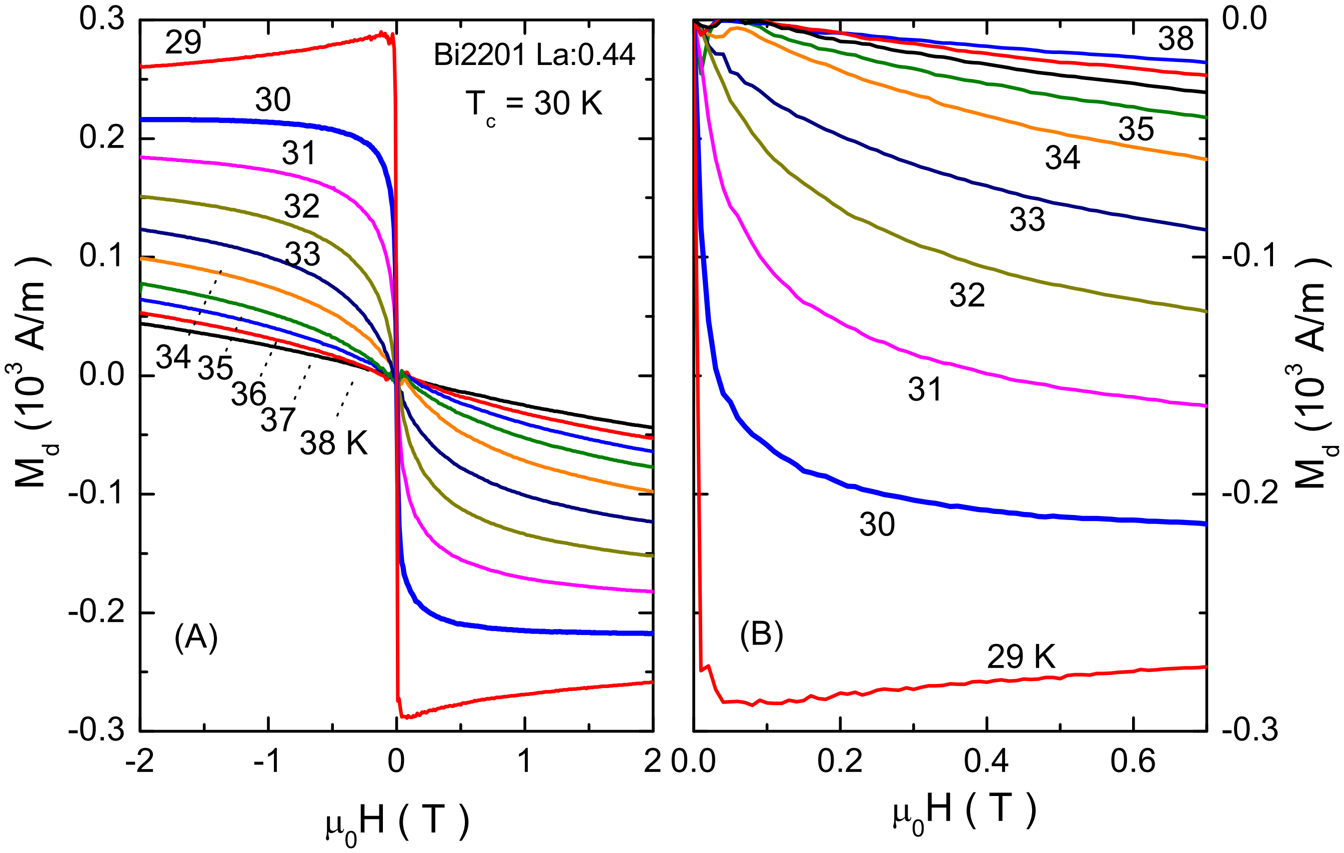

Van Vleck background $(A + BT)H$ *is subtracted*

$T_c = 30K$

Enhanced diamagnetism of $Bi_2Sr_{2-y}La_yCuO_6$ samples with $y = 0.44$ content of La atoms.

Torque magnetometry

evidence for diamagnetism above T_c

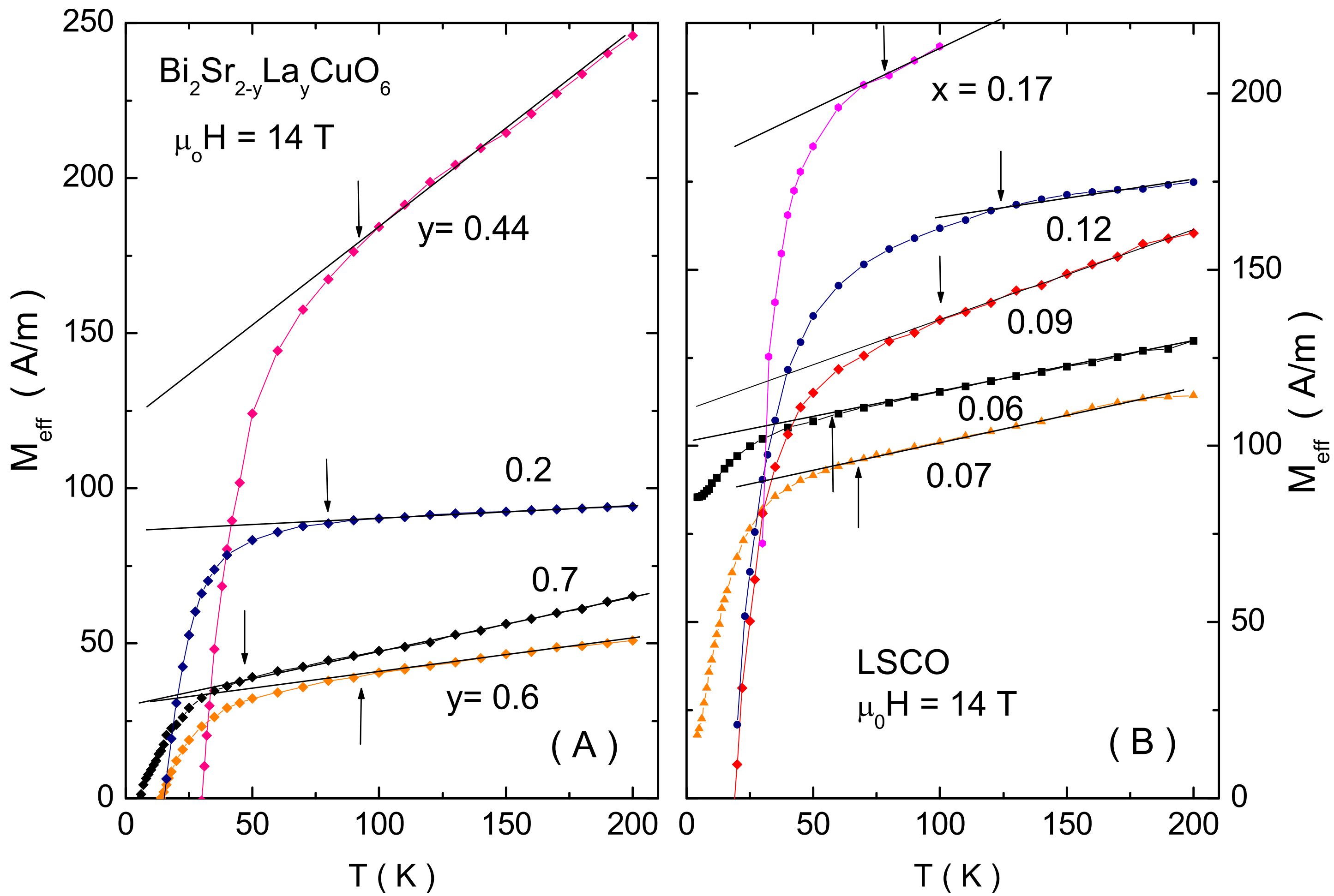

Magnetisation of $La_{2-x}Sr_xCuO_4$ and $Bi_2Sr_{2-y}La_yCuO_6$ samples, showing the onset of doping dependent diamagnetism above T_c.

Torque magnetometry

evidence for diamagnetism above T_c

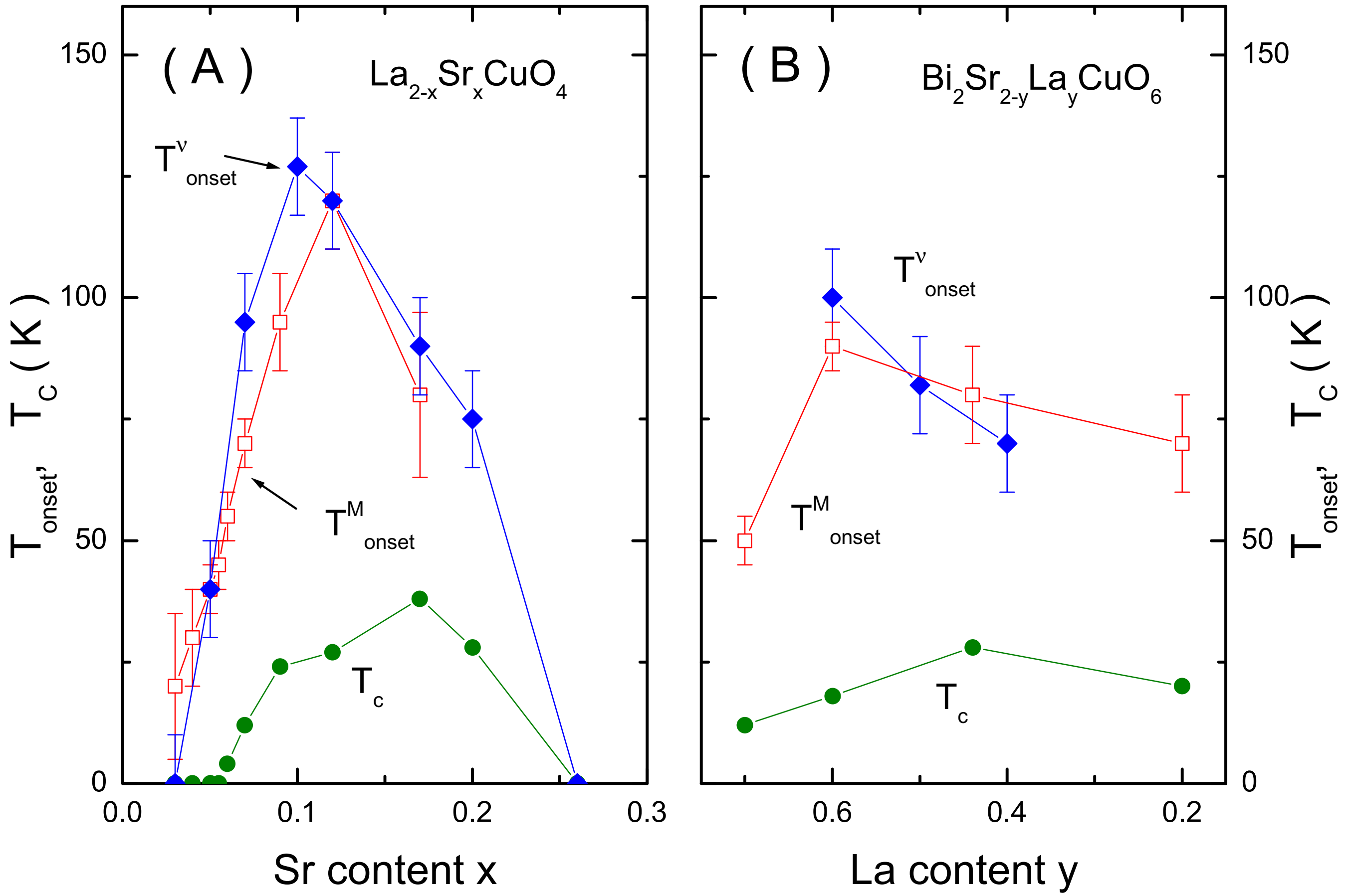

T^M ⟸ **onset of the residual diamagnetism**

T_c ⟸ **transition to superconducting state**

L. Li, ... and N.P. Ong, Phys. Rev. B **81**, *054510 (2010).*

Issues to be addressed:

Issues to be addressed:

★ **Why does T^M differ from T_c ?**

/ pairing vs coherence /

Issues to be addressed:

- **Why does T^M differ from T_c ?**

  / pairing vs coherence /

- **Meissner without Higgs mechanism ?**

Issues to be addressed:

★ **Why does T^M differ from T_c ?**

/ pairing vs coherence /

★ **Meissner without Higgs mechanism ?**

$\Rightarrow$ *Diamagnetism above T_c*

Issues to be addressed:

★ **Why does T^M differ from T_c ?**

/ pairing vs coherence /

★ **Meissner without Higgs mechanism ?**

- *Diamagnetism above T_c*

$\Rightarrow$ *Enhanced conductivity above T_c*

Issues to be addressed:

★ **Why does T^M differ from T_c ?**

/ pairing vs coherence /

★ **Meissner without Higgs mechanism ?**

- *Diamagnetism above* T_c
- *Enhanced conductivity above* T_c

★ **General remarks**

Superconducting state – principal features

Superconducting state – principal features

★ **ideal d.c. conductance**

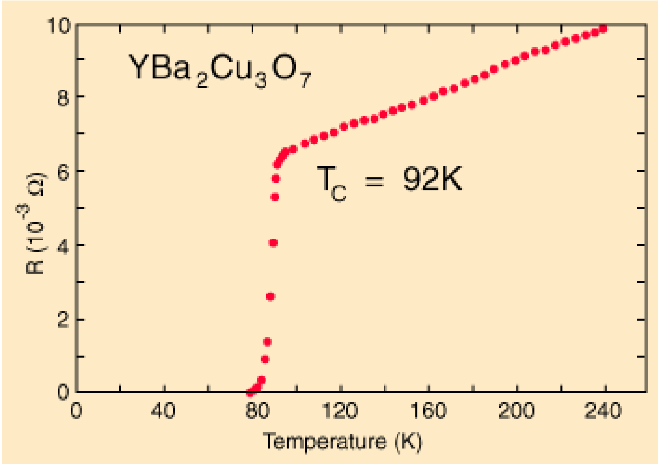

Superconducting state – principal features

★ **ideal d.c. conductance**

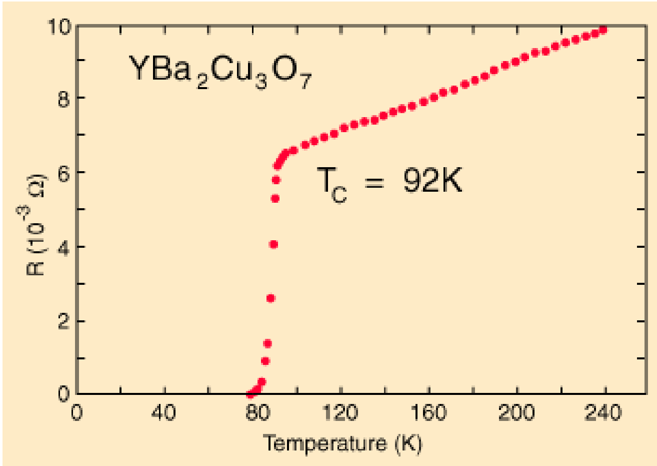

Normal conductors:

resistance $R = \rho \, \frac{l}{S}$

where $\rho \equiv 1/\sigma$

and $\sigma = \frac{ne^2\tau}{m}$

$\tau(T)$ **– relaxation time**

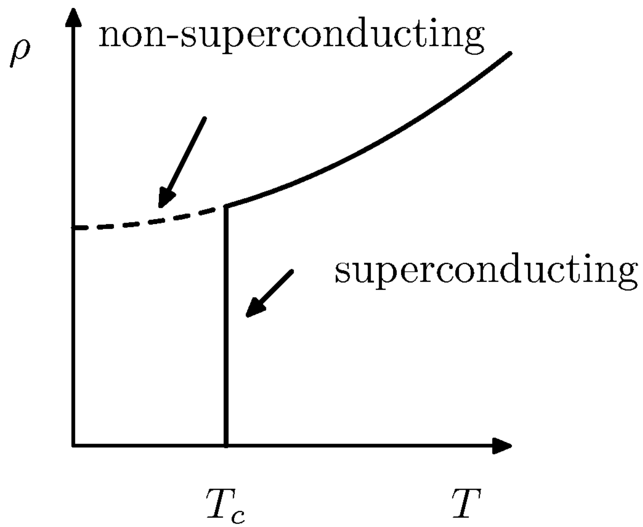

Superconducting state – principal features

★ **ideal d.c. conductance**

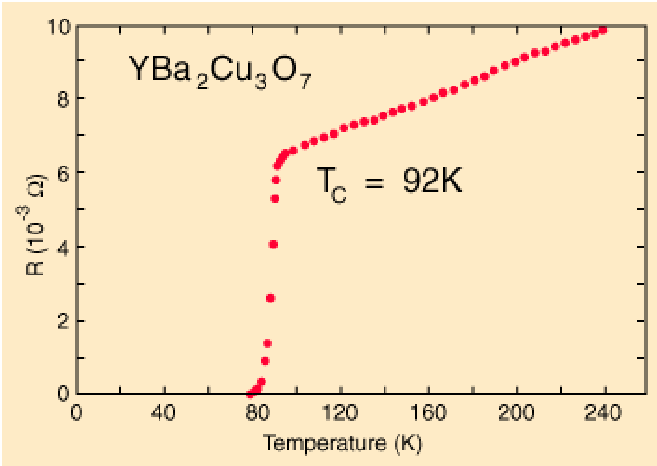

a.c. conductance

Drude conductance

$$\sigma(\omega) = \frac{ne^2\tau}{m} \frac{1}{1-i\omega\tau}$$

obeys the f-sum rule

$$\int_{-\infty}^{\infty} \mathrm{Re}\, \sigma(\omega) = \pi \frac{ne^2}{m}$$

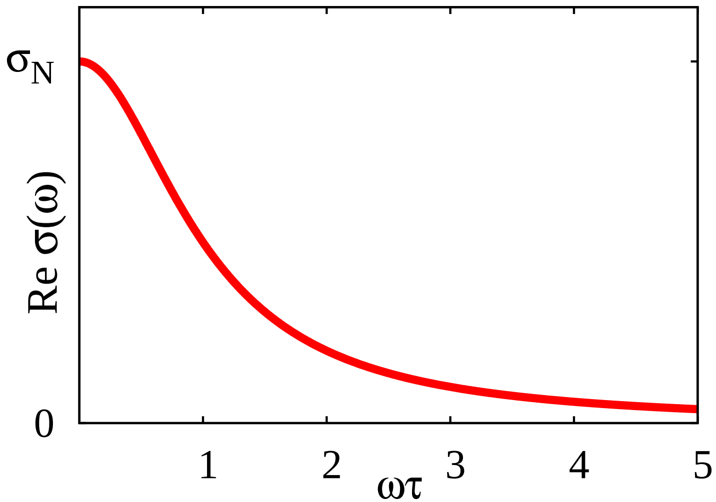

Superconducting state – principal features

★ **ideal d.c. conductance**

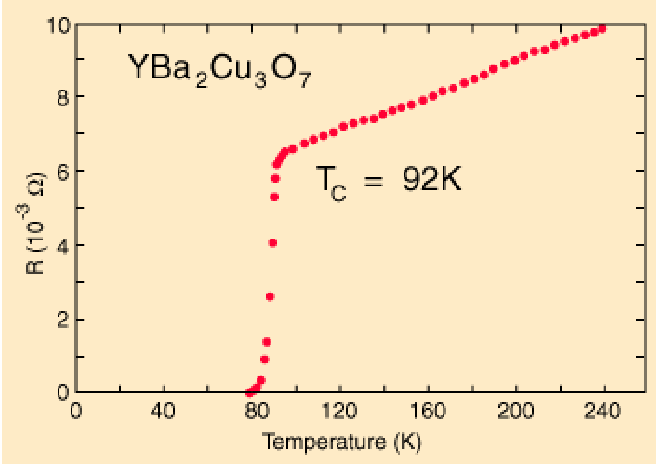

a.c. conductance

This f-sum rule

$$\int_{-\infty}^{\infty} \mathrm{Re}\ \sigma(\omega) = \pi\ \frac{ne^2}{m}$$

must be obeyed also below T_c, where

$$\boldsymbol{n = n_n + n_s}$$

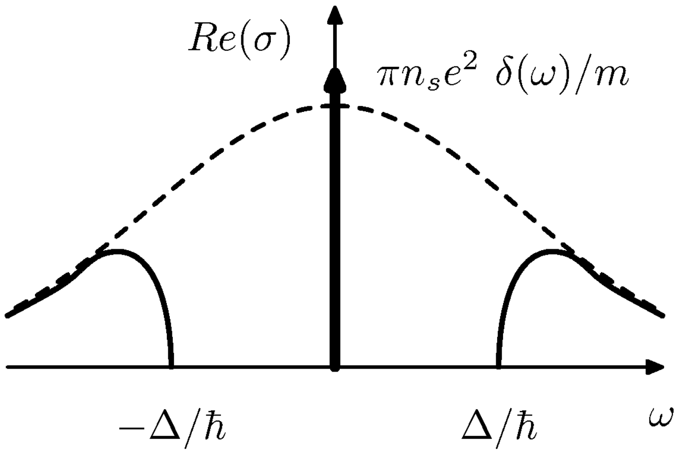

n_s – **superfluid density**

Superconducting state – properties (continued)

Superconducting state – properties (continued)

* **ideal diamagnetism** /perfect screening of d.c. magnetic field/

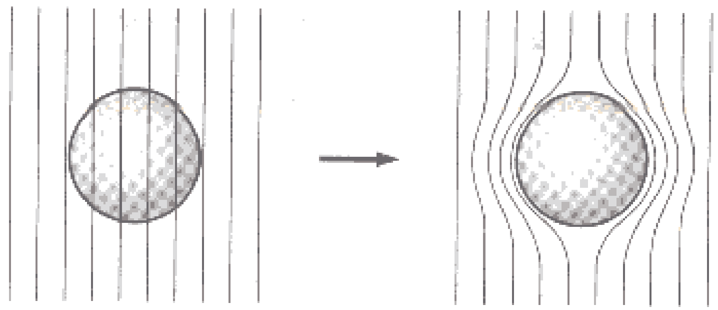

$T > T_c$ $\qquad$ $T < T_c$

Superconducting state – properties (continued)

★ **ideal diamagnetism** /perfect screening of d.c. magnetic field/

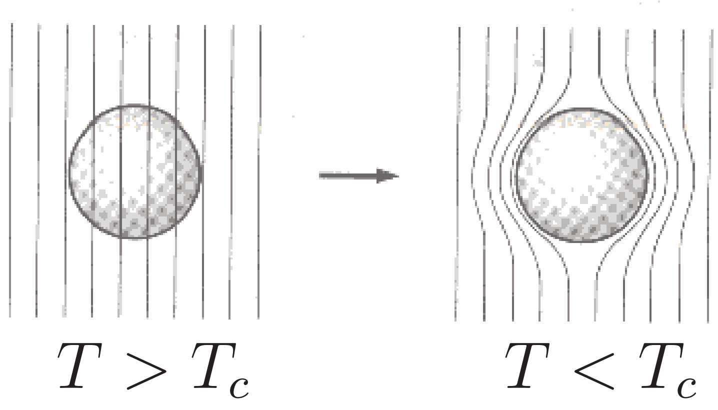

Meissner effect is described by the Londons' equation

$$\vec{j} = - \frac{e^2 n_s(T)}{mc^2} \vec{A}$$

where the coefficient

$$\frac{e^2 n_s(T)}{mc^2} \equiv \rho_s(T) = \frac{1}{\lambda^2}$$

$\rho_s(T)$ **– superfluid stiffness**

$\lambda(T)$ – penetration depth

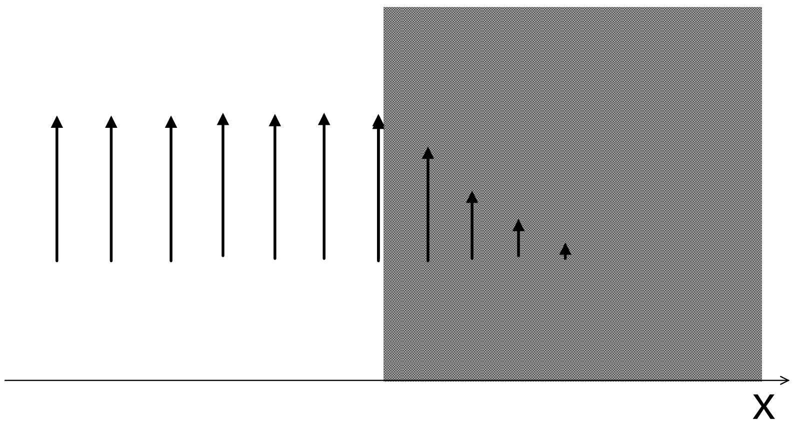

$$B(x) = B_0 e^{-x/\lambda}$$

Superconducting state – basic concepts

Superconducting state – basic concepts

⇛ **ideal d.c. conductance**

Superconducting state – basic concepts

⇒ **ideal d.c. conductance**

⇒ **ideal diamagnetism (Meissner effect)**

Superconducting state – basic concepts

- ⇛ **ideal d.c. conductance**
- ⇛ **ideal diamagnetism (Meissner effect)**

can be regarded as two sides of the same coin.

Superconducting state – basic concepts

- $\Longrightarrow$ ideal d.c. conductance
- $\Longrightarrow$ ideal diamagnetism (Meissner effect)

can be regarded as two sides of the same coin.

Both effects are caused by the superfluid fraction

$$n_s(T)$$

Formal issues

Formal issues

The order parameter

$$\chi \equiv \langle \hat{c}_{\downarrow}(\vec{r}_i)\hat{c}_{\uparrow}(\vec{r}_j)\rangle$$

Formal issues

The order parameter

$$\chi \equiv \langle \hat{c}_{\downarrow}(\vec{r}_i)\hat{c}_{\uparrow}(\vec{r}_j)\rangle$$

is a complex quantity

$$\chi = |\chi| \, e^{i\theta}$$

Formal issues

The order parameter

$$\chi \equiv \langle \hat{c}_{\downarrow}(\vec{r}_i)\hat{c}_{\uparrow}(\vec{r}_j)\rangle$$

is a complex quantity

$$\chi = |\chi| \, e^{i\theta}$$

It has the following physical implications:

Formal issues

The order parameter

$$\chi \equiv \langle \hat{c}_{\downarrow}(\vec{r}_i)\hat{c}_{\uparrow}(\vec{r}_j)\rangle$$

is a complex quantity

$$\chi = |\chi| \, e^{i\theta}$$

It has the following physical implications:

$|\chi| \neq 0 \longrightarrow$ **amplitude causes the energy gap**

Formal issues

The order parameter

$$\chi \equiv \langle \hat{c}_{\downarrow}(\vec{r}_i)\hat{c}_{\uparrow}(\vec{r}_j)\rangle$$

is a complex quantity

$$\chi = |\chi| \, e^{i\theta}$$

It has the following physical implications:

$|\chi| \neq 0 \longrightarrow$ **amplitude causes the energy gap**

$\nabla\theta \neq 0 \longrightarrow$ **phase slippage induces supercurrents**

Critical temperature – amplitude vs phase transition

Critical temperature – amplitude vs phase transition

The complex order parameter

$$\chi = |\chi| \, e^{i\theta}$$

Critical temperature – amplitude vs phase transition

The complex order parameter

$$\chi = |\chi| \, e^{i\theta}$$

can vanish at $T \longrightarrow T_c$ by:

Critical temperature – amplitude vs phase transition

The complex order parameter

$$\chi = |\chi| \, e^{i\theta}$$

can vanish at $T \longrightarrow T_c$ by:

1. **closing the gap** . . . . **[conventional BCS superconductors]**

$$\lim_{T \to T_c} |\chi| = 0$$

Critical temperature – amplitude vs phase transition

The complex order parameter

$$\chi = |\chi| \, e^{i\theta}$$

can vanish at $T \longrightarrow T_c$ by:

1. **closing the gap** . . . . [conventional BCS superconductors]

$$\lim_{T \to T_c} \ |\chi| = 0$$

2. **randomizing the phase** . . . . [HTSC & disordered thin superconductors]

$$\lim_{T \to T_c} \ \langle \theta \rangle = 0$$

Amplitude vs phase driven transition

scenario # 1

Amplitude vs phase driven transition

scenario # 1

⇒ **amplitude transition** */ classical superconductors /*

$$k_B\, T_c \simeq \frac{\Delta(0)}{1.76}$$

Amplitude vs phase driven transition

scenario # 1

⇒ **amplitude transition** */ classical superconductors /*

$$k_B\, T_c \simeq \frac{\Delta(0)}{1.76}$$

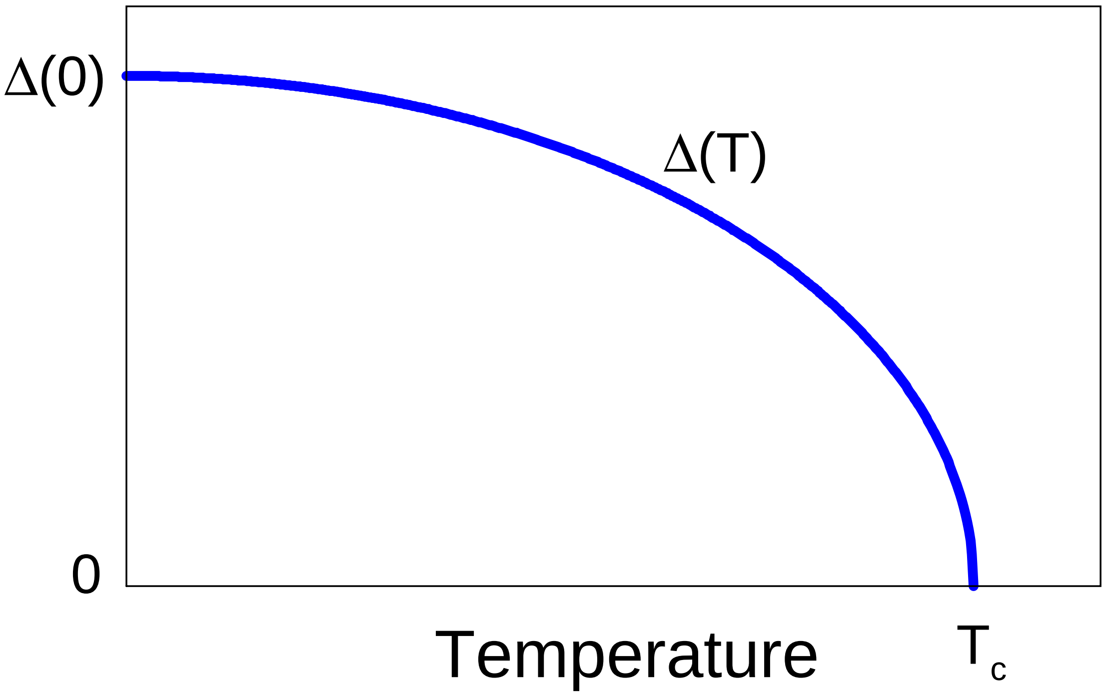

Electrons' pairing is responsible for the energy gap $\boldsymbol{\Delta(T)}$ *in a single particle spectrum*

$$\boldsymbol{\Delta(T_c) = 0}$$

Appearance of the electron pairs is simultaneous with onset of their coherence

Amplitude vs phase driven transition

scenario $\#$ 2

Amplitude vs phase driven transition

scenario # 2

$\Rightarrow$ **phase-driven transition** */ high T_c cuprate oxides /*

$T_c \not\sim \Delta(0)$

Amplitude vs phase driven transition

scenario # 2

⇒ **phase-driven transition** */ high T_c cuprate oxides /* $T_c \not\sim \Delta(0)$

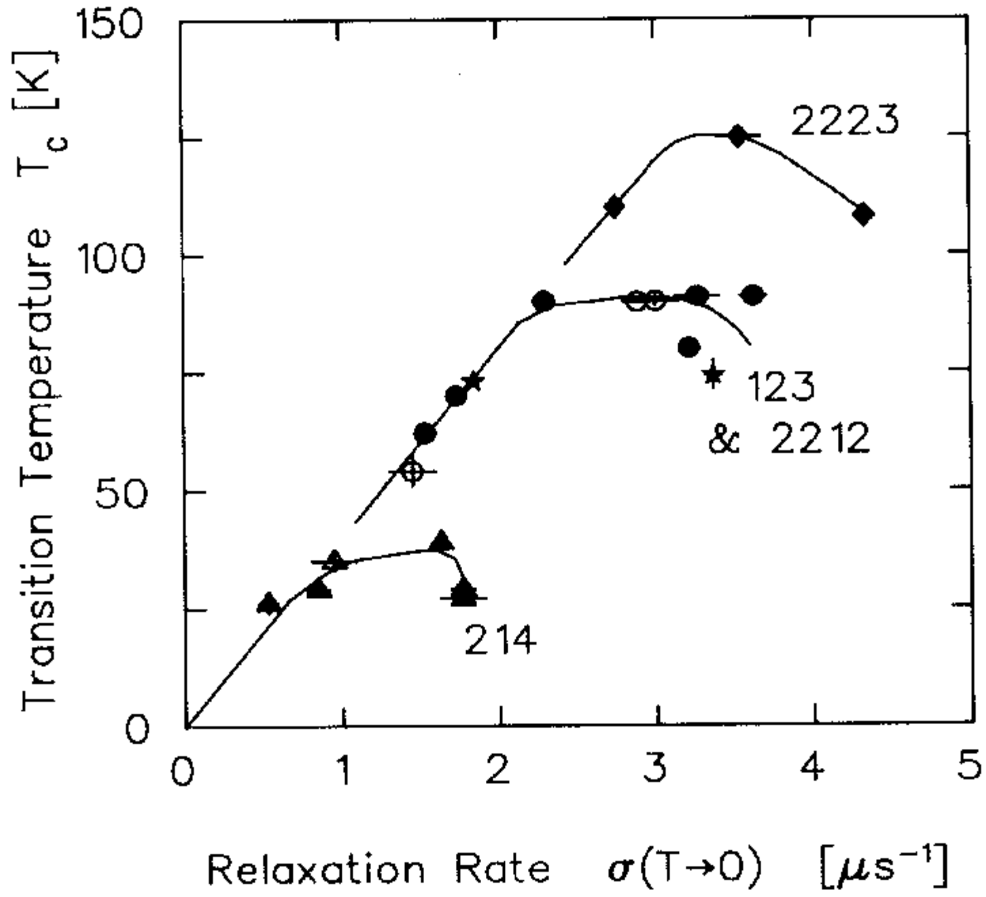

Y.J. Uemura et al, Phys. Rev. Lett. ***62****, 2317 (1989).*

Early experiments using the muon-spin relaxation indicated that in HTSC

$$T_c \propto \rho_s(0)$$

/ Uemura scaling /

The superfluid stiffness $\rho_s(T)$ is here defined by

$$\rho_s(T) \equiv \frac{1}{\lambda^2(T)} = \frac{4\pi e^2}{m^* c^2} n_s(T)$$

Amplitude vs phase driven transition

scenario # 2

⇒ **phase-driven transition** */ high T_c cuprate oxides /*

$T_c \not\sim \Delta(0)$

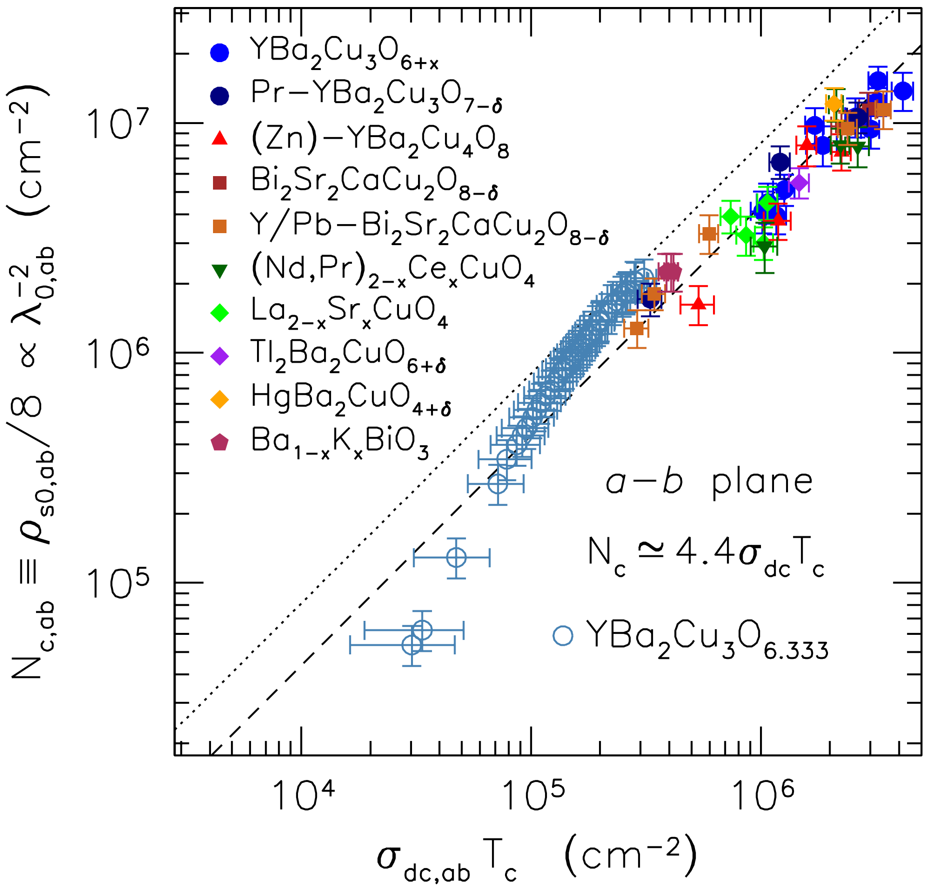

C.C. Homes, Phys. Rev. B ***80****, 180509(R) (2009).*

Recently such scaling has been updated from transport measurements

$$\frac{1}{8}\rho_s = 4.4\sigma_{dc}\,T_c$$

/ Homes scaling /

This new relation is valid for all samples ranging from the underdoped to overdoped region.

/ ab - plane /

Amplitude vs phase driven transition

scenario # 2

⇒ **phase-driven transition** */ high T_c cuprate oxides /*

$T_c \not\sim \Delta(0)$

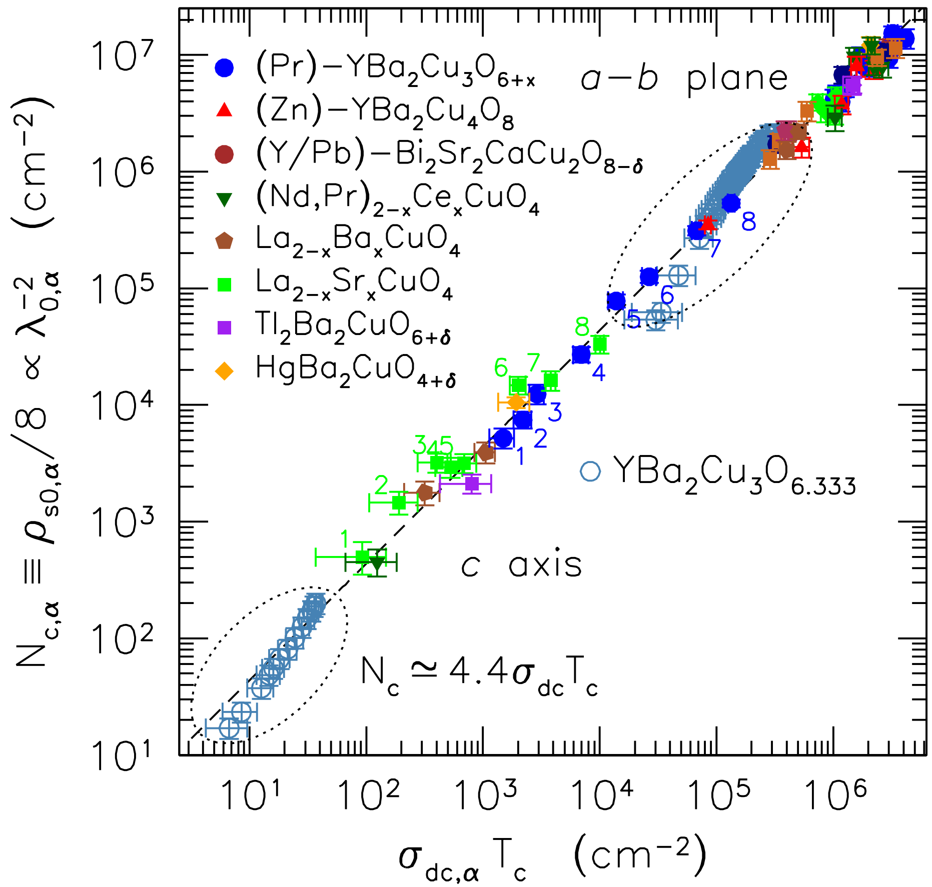

C.C. Homes, Phys. Rev. B **80**, 180509(R) (2009).

Recently such scaling has been updated from transport measurements

$$\frac{1}{8}\rho_s = 4.4\sigma_{dc}\,T_c$$

/ Homes scaling /

This new relation is valid for all samples ranging from the underdoped to overdoped region.

/ c - axis /

Electron ’pre-pairing’

/experimental evidence/

Incoherent pairs above T_c

experimental fact # 1

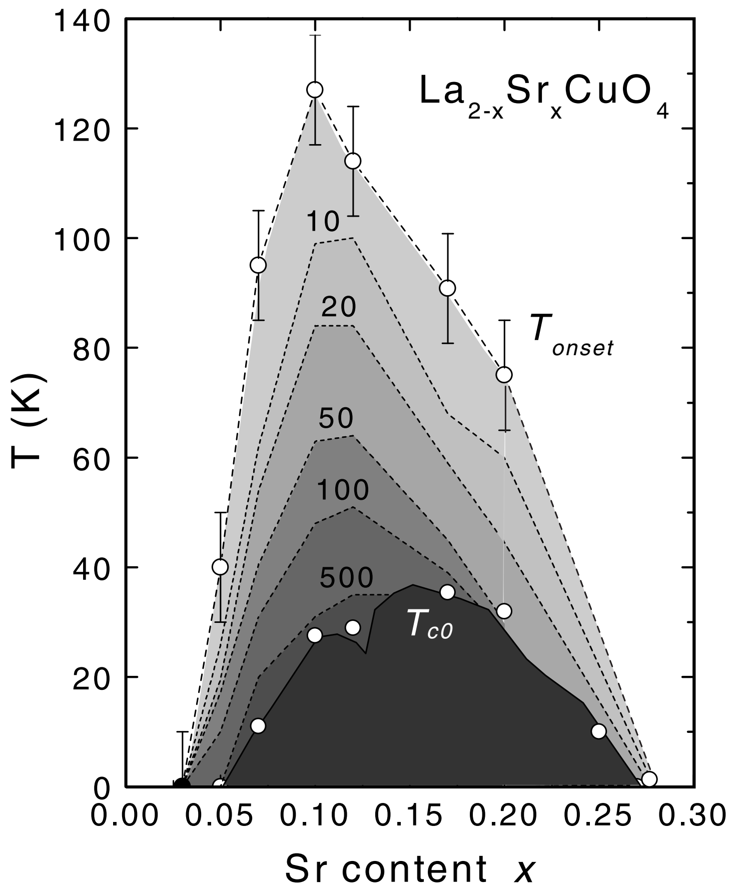

Phase slippage detected in the large Nernst effect.

Y. Wang et al, *Science* **299**, *86 (2003).*

Incoherent pairs above T_c

experimental fact # 1

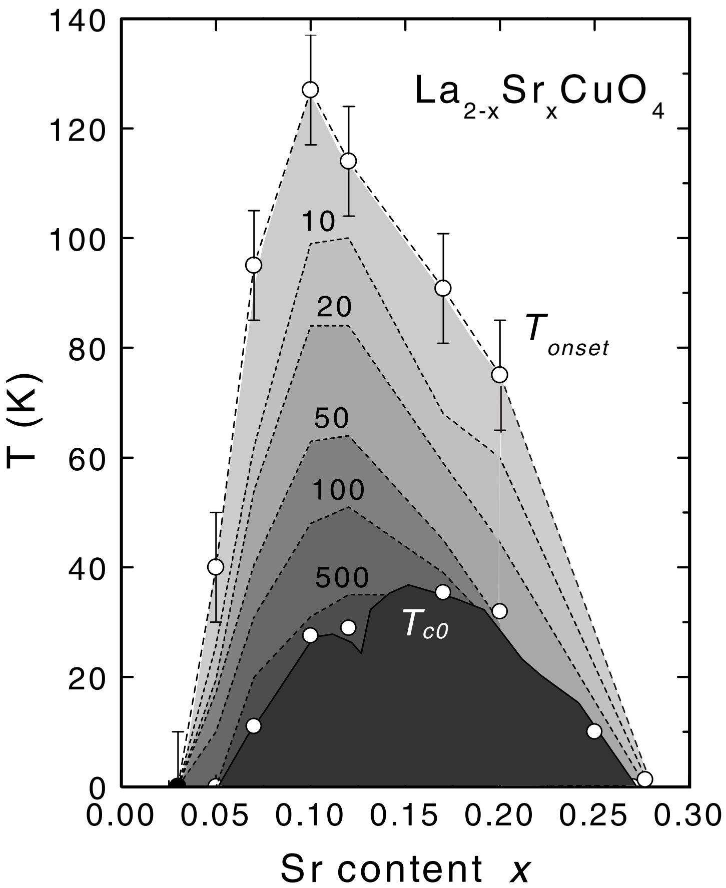

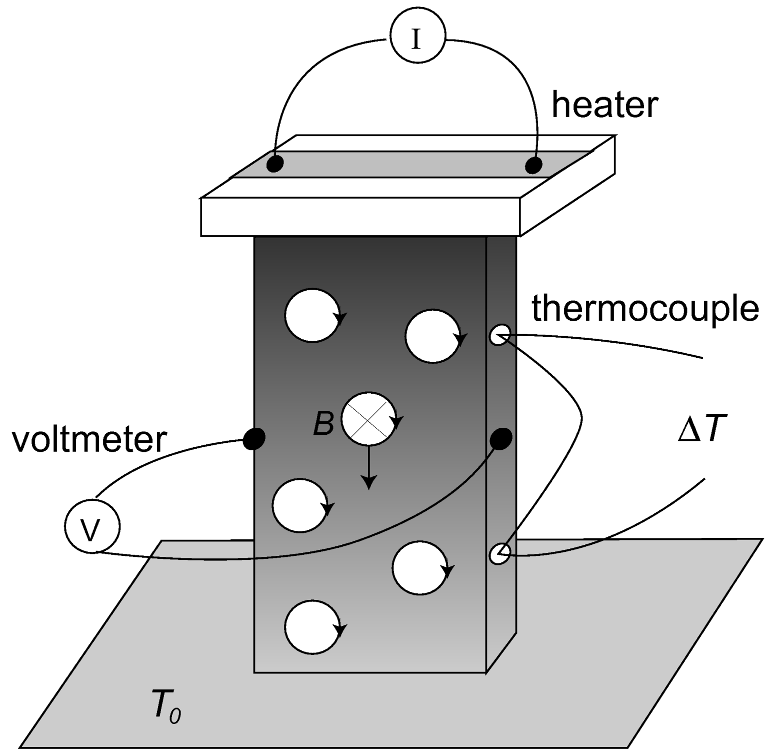

Phase slippage detected in the large Nernst effect.

Y. Wang et al, *Science* **299**, *86 (2003).*

Incoherent pairs above T_c

experimental fact $\#$ 2

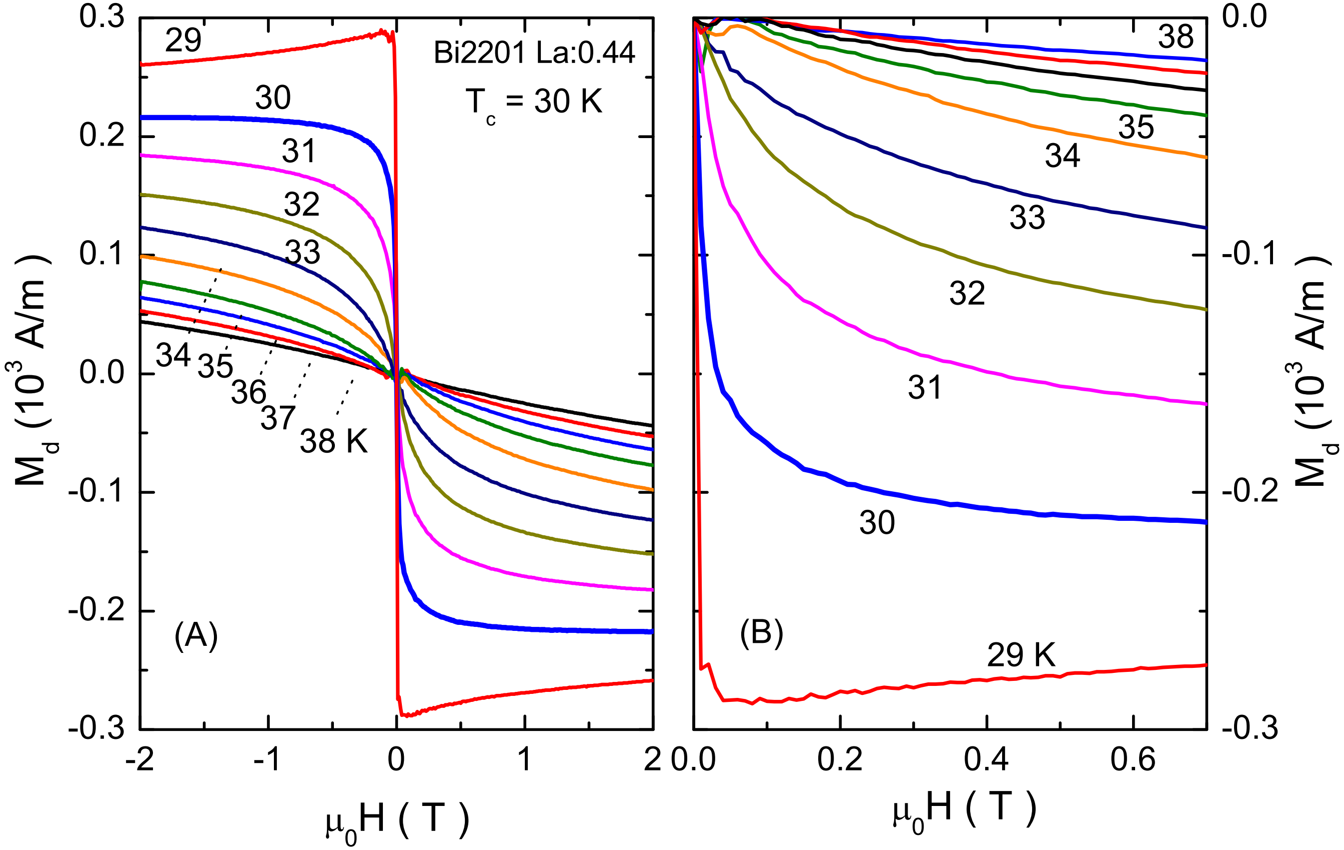

Van Vleck background $(A + BT)H$ *is subracted*

$$T_c = 30K$$

Enhanced diagnetic response revealed above T_c by the high precission torque magnetometry.

L. Li, ... and N.P. Ong, Phys. Rev. B **81**, *054510 (2010).*

/ Princeton University /

Incoherent pairs above T_c

experimental fact # 3

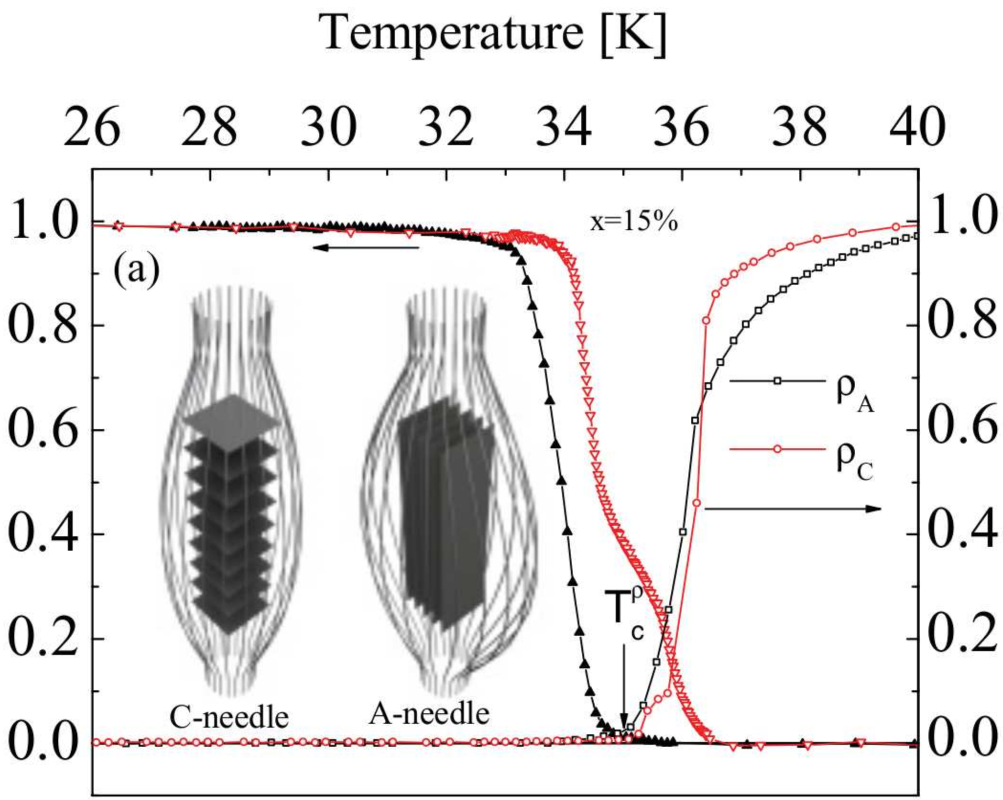

G. Drachuck et al, *Phys. Rev. B* **85**, *184518 (2012).*

/ Technion Group /

Magnetization measurements for the needle shape $La_{2-x}Sr_xCuO_4$ single crystals.

Incoherent pairs above T_c

experimental fact # 4

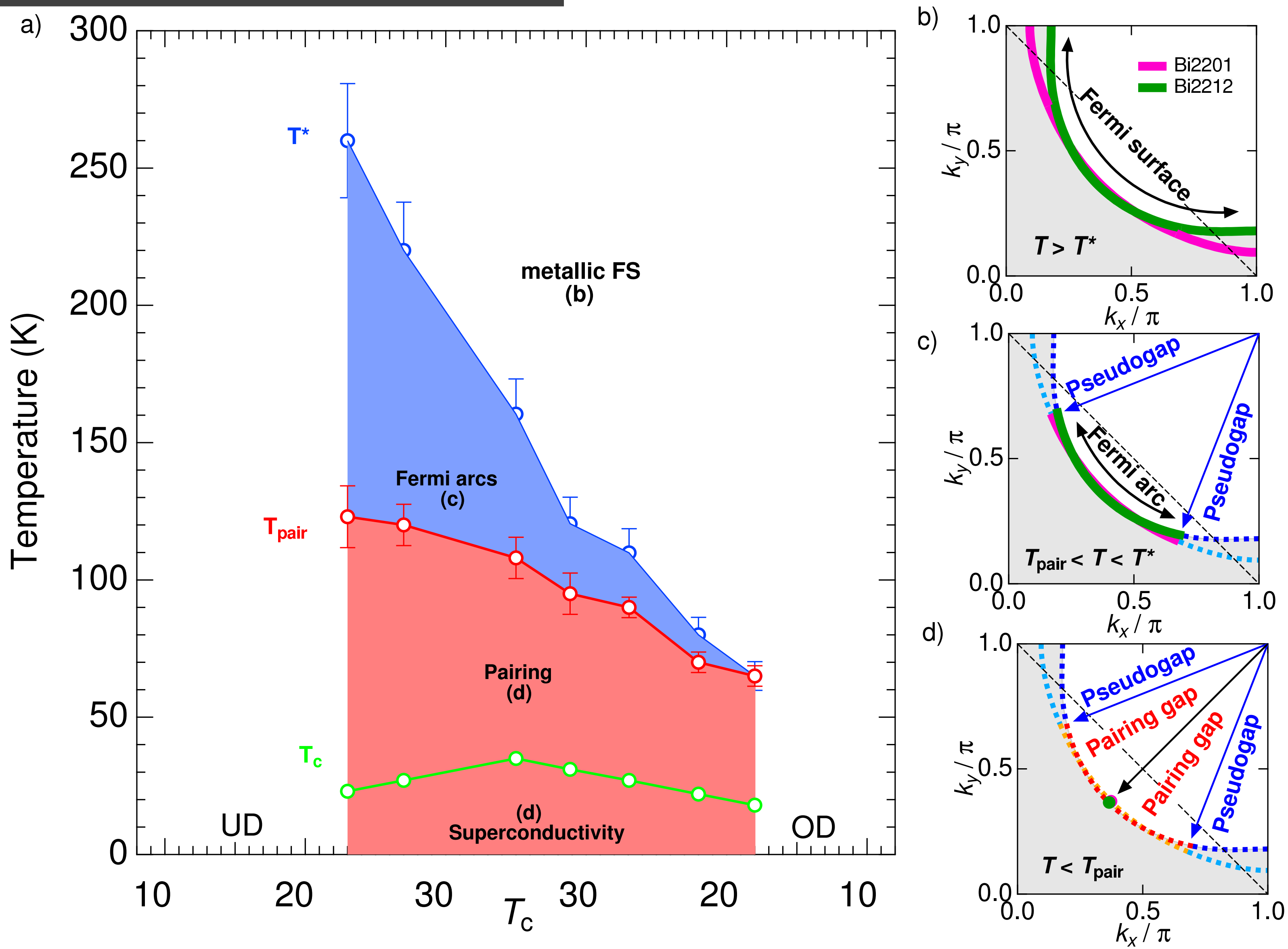

A. Kamiński, T. Kondo, T. Takeuchi, and G. Gu, Phil. Mag. B **95**, 453 (2015).

Incoherent pairs above T_c

experimental fact # 5

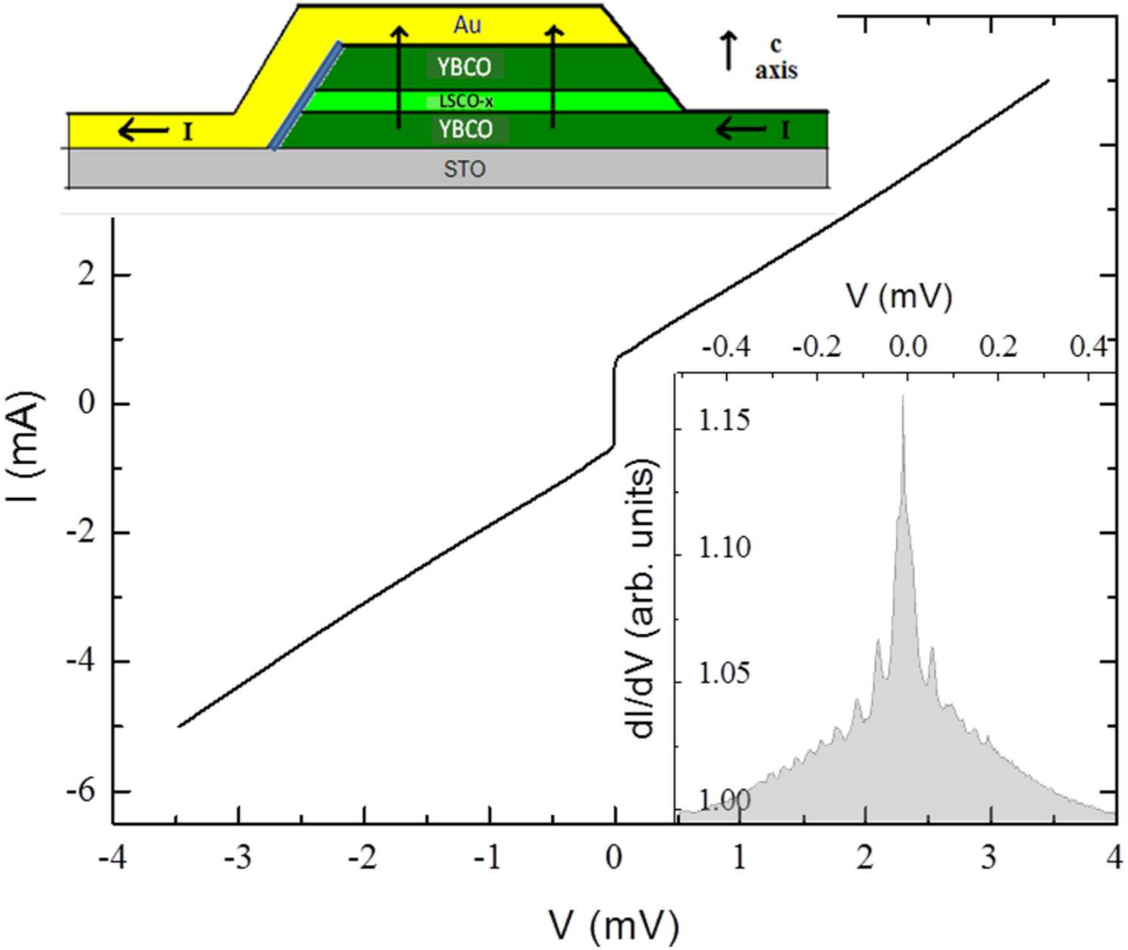

Josephson current in YBaCuO - LaSrCuO - YBaCuO junction with LaSrCuO being in the pseudogap state well above T_c

T. Kirzhner and G. Koren, Scientific Reports **4***, 6244 (2014).*

Incoherent pairs above T_c

experimental fact # 6

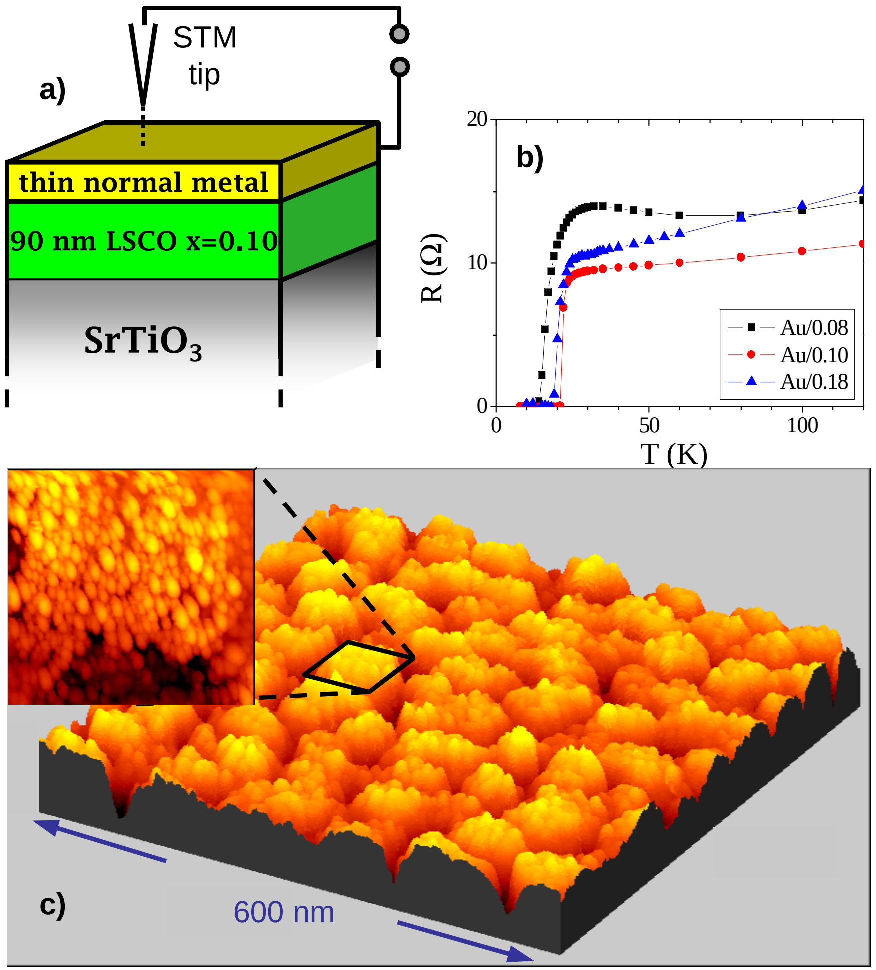

Pseudogap induced well above T_c in ultrathin metallic slab deposited on $La_{2-x}Sr_xCuO_4$.

O. Yuli et al, *Phys. Rev. Lett.* **103**, *197003 (2009).*

Incoherent pairs above T_c

experimental fact # 7

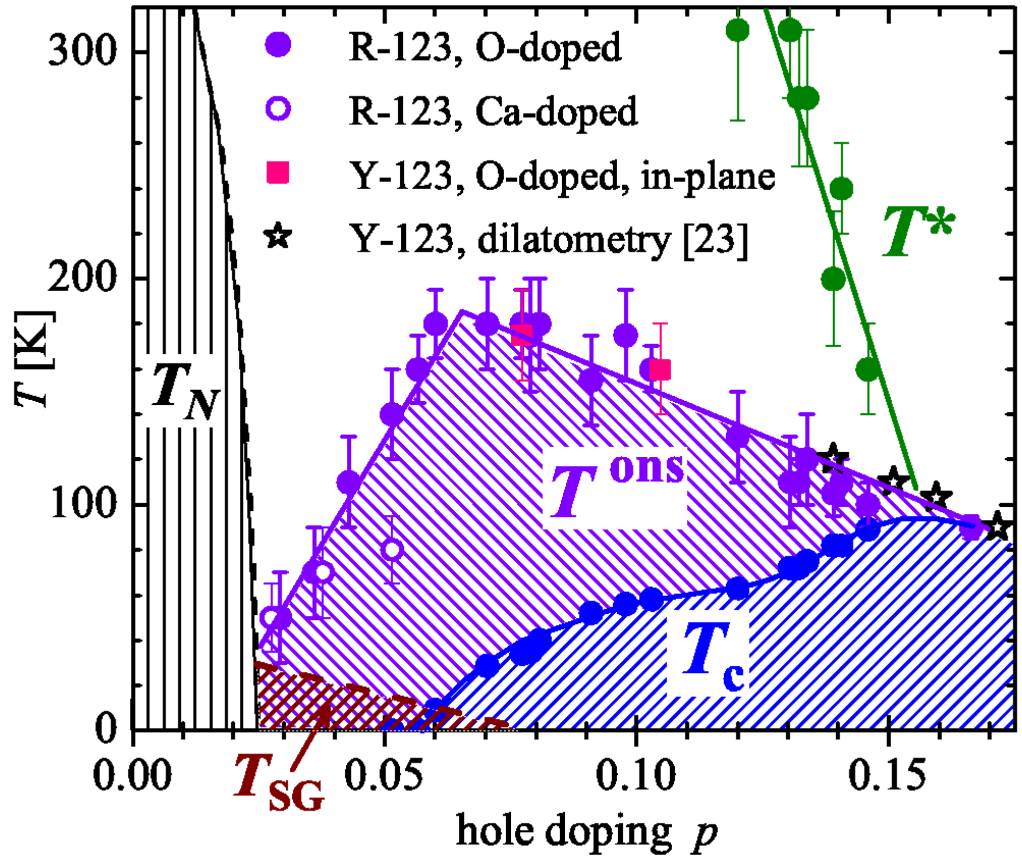

A. Dubroka et al, *Phys. Rev. Lett.* **106**, *047006 (2011).*

Onset of the superfulid fraction observed in the c-axis optical measurements Re$\sigma_c(\omega)$.

Incoherent pairs above T_c

... *continued*

⇒ **Bogoliubov quasiparticles detected above T_c in ARPES measurements for YBaCuO and LaSrCuO compounds**

Argonne (2008), Villigen (2009).

⇒ **Bogoliubov-type interference patterns in pseudogap state as the *fingerprint* of phase incoherent d-wave superconductivity preserved up to 1.5 T_c**

J. Lee, ... and J.C. Davis, Science **325***, 1099 (2009).*

Diamagnetism

and its origin above T_c

Phenomenological model

$$\hat{H} = \sum_{\mathbf{k},\sigma} \xi_{\mathbf{k}} \hat{c}^{\dagger}_{\mathbf{k}\sigma} \hat{c}_{\mathbf{k}\sigma} + \sum_{\mathbf{q}} E_{\mathbf{q}} \hat{b}^{\dagger}_{\mathbf{q}} \hat{b}_{\mathbf{q}} + \sum_{\mathbf{k},\mathbf{p}} g_{\mathbf{k},\mathbf{p}} \left(\hat{b}^{\dagger}_{\mathbf{k}+\mathbf{p}} \hat{c}_{\mathbf{k}\downarrow} \hat{c}_{\mathbf{p}\uparrow} + \hat{b}_{\mathbf{k}+\mathbf{p}} \hat{c}^{\dagger}_{\mathbf{k}\uparrow} \hat{c}^{\dagger}_{\mathbf{p}\downarrow} \right)$$

This Hamiltonian describes a two-component system consisting of:

$\hat{c}^{(\dagger)}_{\mathbf{k}\sigma}$ itinerant fermions . . . . *(e.g. holes near the Mott insulator)*

Phenomenological model

$$\hat{H} = \sum_{\mathbf{k},\sigma} \xi_{\mathbf{k}} \hat{c}^{\dagger}_{\mathbf{k}\sigma} \hat{c}_{\mathbf{k}\sigma} + \sum_{\mathbf{q}} E_{\mathbf{q}} \hat{b}^{\dagger}_{\mathbf{q}} \hat{b}_{\mathbf{q}} + \sum_{\mathbf{k},\mathbf{p}} g_{\mathbf{k},\mathbf{p}} \left(\hat{b}^{\dagger}_{\mathbf{k}+\mathbf{p}} \hat{c}_{\mathbf{k}\downarrow} \hat{c}_{\mathbf{p}\uparrow} + \hat{b}_{\mathbf{k}+\mathbf{p}} \hat{c}^{\dagger}_{\mathbf{k}\uparrow} \hat{c}^{\dagger}_{\mathbf{p}\downarrow} \right)$$

This Hamiltonian describes a two-component system consisting of:

- $\hat{c}^{(\dagger)}_{\mathbf{k}\sigma}$ itinerant fermions . . . . *(e.g. holes near the Mott insulator)*
- $\hat{b}^{(\dagger)}_{\mathbf{q}}$ preformed local pairs . . . . *(RVB defines them on the bonds)*

Phenomenological model

$$\hat{H} = \sum_{\mathbf{k},\sigma} \xi_{\mathbf{k}} \hat{c}^\dagger_{\mathbf{k}\sigma} \hat{c}_{\mathbf{k}\sigma} + \sum_{\mathbf{q}} E_{\mathbf{q}} \hat{b}^\dagger_{\mathbf{q}} \hat{b}_{\mathbf{q}}$$
$$+ \sum_{\mathbf{k},\mathbf{p}} g_{\mathbf{k},\mathbf{p}} \left(\hat{b}^\dagger_{\mathbf{k}+\mathbf{p}} \hat{c}_{\mathbf{k}\downarrow} \hat{c}_{\mathbf{p}\uparrow} + \hat{b}_{\mathbf{k}+\mathbf{p}} \hat{c}^\dagger_{\mathbf{k}\uparrow} \hat{c}^\dagger_{\mathbf{p}\downarrow} \right)$$

This Hamiltonian describes a two-component system consisting of:

$\hat{c}^{(\dagger)}_{\mathbf{k}\sigma}$ itinerant fermions . . . . *(e.g. holes near the Mott insulator)*

$\hat{b}^{(\dagger)}_{\mathbf{q}}$ preformed local pairs . . . . *(RVB defines them on the bonds)*

interacting via:

Phenomenological model

$$\hat{H} = \sum_{\mathbf{k},\sigma} \xi_{\mathbf{k}} \hat{c}^{\dagger}_{\mathbf{k}\sigma} \hat{c}_{\mathbf{k}\sigma} + \sum_{\mathbf{q}} E_{\mathbf{q}} \hat{b}^{\dagger}_{\mathbf{q}} \hat{b}_{\mathbf{q}} + \sum_{\mathbf{k},\mathbf{p}} g_{\mathbf{k},\mathbf{p}} \left(\hat{b}^{\dagger}_{\mathbf{k}+\mathbf{p}} \hat{c}_{\mathbf{k}\downarrow} \hat{c}_{\mathbf{p}\uparrow} + \hat{b}_{\mathbf{k}+\mathbf{p}} \hat{c}^{\dagger}_{\mathbf{k}\uparrow} \hat{c}^{\dagger}_{\mathbf{p}\downarrow} \right)$$

This Hamiltonian describes a two-component system consisting of:

$\hat{c}^{(\dagger)}_{\mathbf{k}\sigma}$ itinerant fermions .... *(e.g. holes near the Mott insulator)*

$\hat{b}^{(\dagger)}_{\mathbf{q}}$ preformed local pairs .... *(RVB defines them on the bonds)*

interacting via:

$\hat{b}^{\dagger}_{\mathbf{q}} \hat{c}_{\mathbf{q}-\mathbf{k},\downarrow} \hat{c}_{\mathbf{k},\uparrow} + h.c.$ .... *(the Andreev-type scattering)*

Response to the external fields

Within the Kubo formalism a response to the electromagnetic field is characterized by the current-current correlation function

$$-\hat{T}_{\tau}\langle \hat{j}_{\mathbf{q}}(\tau)\, \hat{j}_{-\mathbf{q}}(0)\rangle$$

where

$$\langle \ldots \rangle = \mathrm{Tr}\left\{ e^{-\beta\hat{H}} \ldots \right\} / \mathrm{Tr}\left\{ e^{-\beta\hat{H}} \right\}$$

and $\beta = 1/k_B T$.

We have diagonalized Hamiltonian by the continuous unitary transformation

$$\begin{aligned}
\mathrm{Tr}\left\{ e^{-\beta\hat{H}}\hat{O} \right\} &= \mathrm{Tr}\left\{ e^{\hat{S}(l)} e^{-\beta\hat{H}} \hat{O} e^{-\hat{S}(l)} \right\} \\
&= \mathrm{Tr}\left\{ e^{\hat{S}(l)} e^{-\beta\hat{H}} e^{-\hat{S}(l)} e^{\hat{S}(l)} \hat{O} e^{-\hat{S}(l)} \right\} \\
&= \mathrm{Tr}\left\{ e^{-\beta\hat{H}(l)} \hat{O}(l) \right\}
\end{aligned}$$

where

$$\hat{H}(l) = e^{\hat{S}(l)}\hat{H}e^{-\hat{S}(l)} \qquad \hat{O}(l) = e^{\hat{S}(l)}\hat{O}e^{-\hat{S}(l)}$$

Technicalities

The initial current operator

$$\hat{j}_{\mathbf{q},\sigma} = \sum_{\mathbf{k}} \mathrm{v}_{\mathbf{k}+\frac{\mathbf{q}}{2}} \hat{c}^{\dagger}_{\mathbf{k},\sigma} \hat{c}_{\mathbf{k}+\mathbf{q},\sigma}$$

has been found (from the flow equation) as

$$\hat{\mathbf{j}}_{\mathbf{q},\uparrow}\ (l) = \sum_{\mathbf{k}} \mathrm{v}_{\mathbf{k}+\frac{\mathbf{q}}{2}} \left(\mathcal{A}_{\mathbf{k},\mathbf{q}}(l) \hat{c}^{\dagger}_{\mathbf{k},\uparrow}\ \hat{c}_{\mathbf{k}+\mathbf{q},\uparrow} + \mathcal{B}_{\mathbf{k},\mathbf{q}}(l) \hat{c}_{-\mathbf{k},\downarrow} \hat{c}^{\dagger}_{-(\mathbf{k}+\mathbf{q}),\downarrow} \right.$$
$$\left. + \sum_{\mathbf{p}} \left(\mathcal{D}_{\mathbf{k},\mathbf{p},\mathbf{q}}(l) \hat{b}_{\mathbf{k}+\mathbf{p}} \hat{c}^{\dagger}_{\mathbf{k},\uparrow}\ \hat{c}^{\dagger}_{\mathbf{p}-\mathbf{q},\downarrow} + \mathcal{F}_{\mathbf{k},\mathbf{p},\mathbf{q}}(l) \hat{b}^{\dagger}_{\mathbf{k}+\mathbf{p}} \hat{c}_{\mathbf{p},\downarrow} \hat{c}_{\mathbf{k}+\mathbf{q},\uparrow} \right) \right)$$

with the boundary conditions

$$\mathcal{A}_{\mathbf{k},\mathbf{q}}(0) = 1 \quad \textbf{and} \quad \mathcal{B}_{\mathbf{k},\mathbf{q}}(0) = \mathcal{D}_{\mathbf{k},\mathbf{p},\mathbf{q}}(0) = \mathcal{F}_{\mathbf{k},\mathbf{p},\mathbf{q}}(0) = 0$$

We next determined the asymptotic values $\lim_{l\to\infty} \mathcal{A}_{\mathbf{k},\mathbf{q}}(l) \equiv \tilde{\mathcal{A}}_{\mathbf{k},\mathbf{q}}$ **from the coupled set of flow equations**

$$\frac{\partial}{\partial l}\mathcal{A}_{\mathbf{k},\mathbf{q}}(l)\ ,\quad \frac{\partial}{\partial l}\mathcal{B}_{\mathbf{k},\mathbf{q}}(l)\ ,\quad \frac{\partial}{\partial l}\mathcal{D}_{\mathbf{k},\mathbf{p},\mathbf{q}}(l)\ ,\quad \frac{\partial}{\partial l}\mathcal{F}_{\mathbf{k},\mathbf{p},\mathbf{q}}(l).$$

Technicalities

The current-current response function

$$- \hat{T}_\tau \langle \hat{j}_{\mathbf{q}}(\tau)\ \hat{j}_{-\mathbf{q}} \rangle \equiv \Pi(\mathbf{q}, \tau)$$

consists the following contributions

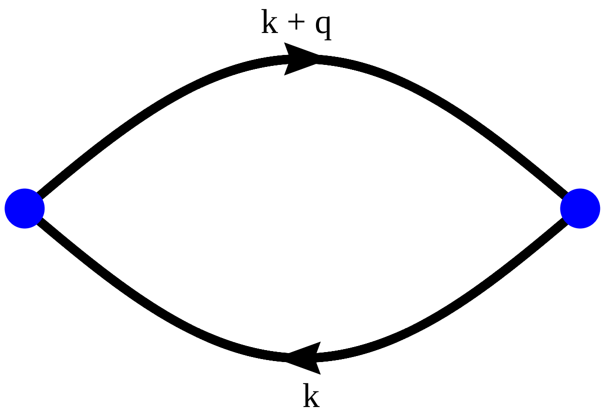

$\Longleftarrow$ **the usual bubble diagram**

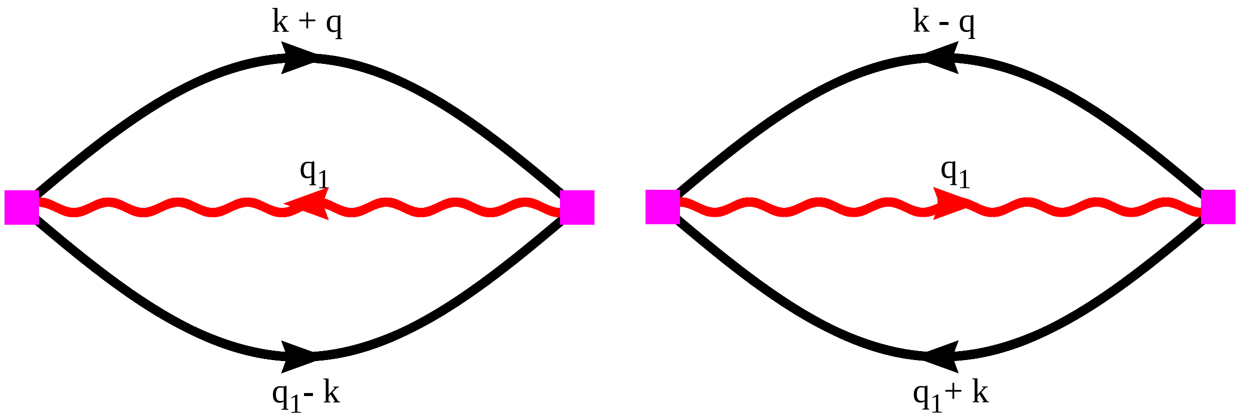

$\Longleftarrow$ **anomalous diagrams**

where each vertex must be determined from the flow equations.

Diagmagnetic response above T_c

The anomalous contributions

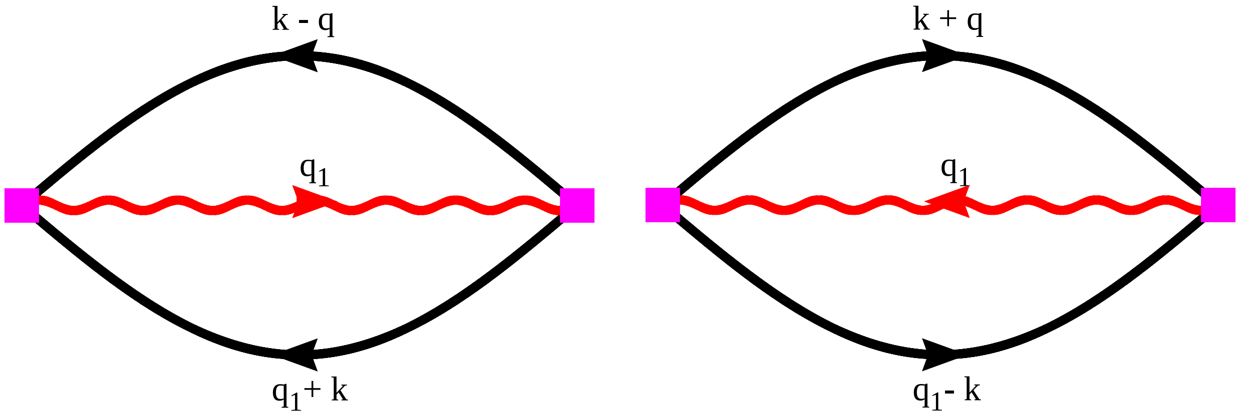

resemble the Aslamasov-Larkin diagram

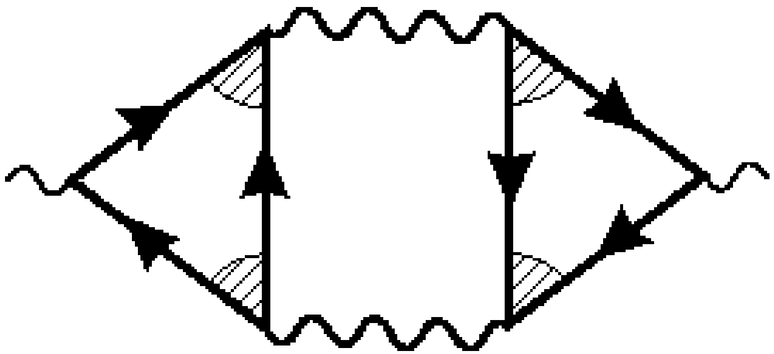

They substantially enhance the conductance/diamagnetism above T_c.

Onset of diamagnetism above T_c

Onset of diamagnetism above T_c

Onset of the diamagnetism is driven by the low-momentum preformed pairs.

Onset of diamagnetism above T_c

Onset of the diamagnetism is driven by the low-momentum preformed pairs.

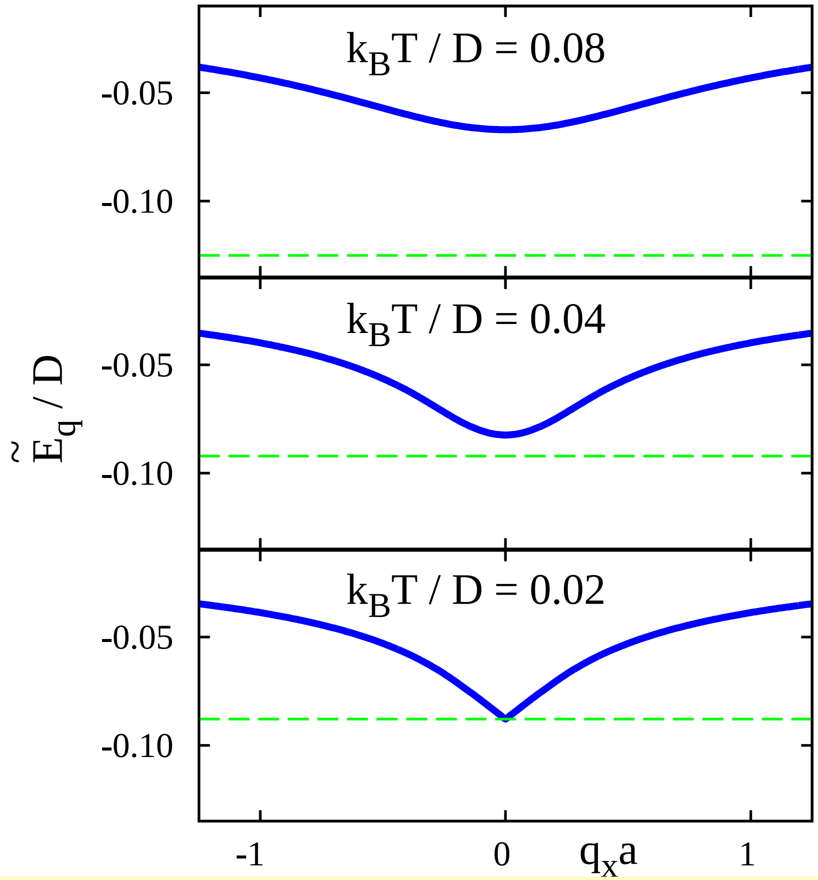

Qulitative changes of the preformed pairs' dispersion.

Onset of diamagnetism above T_c

Onset of the diamagnetism is driven by the low-momentum preformed pairs.

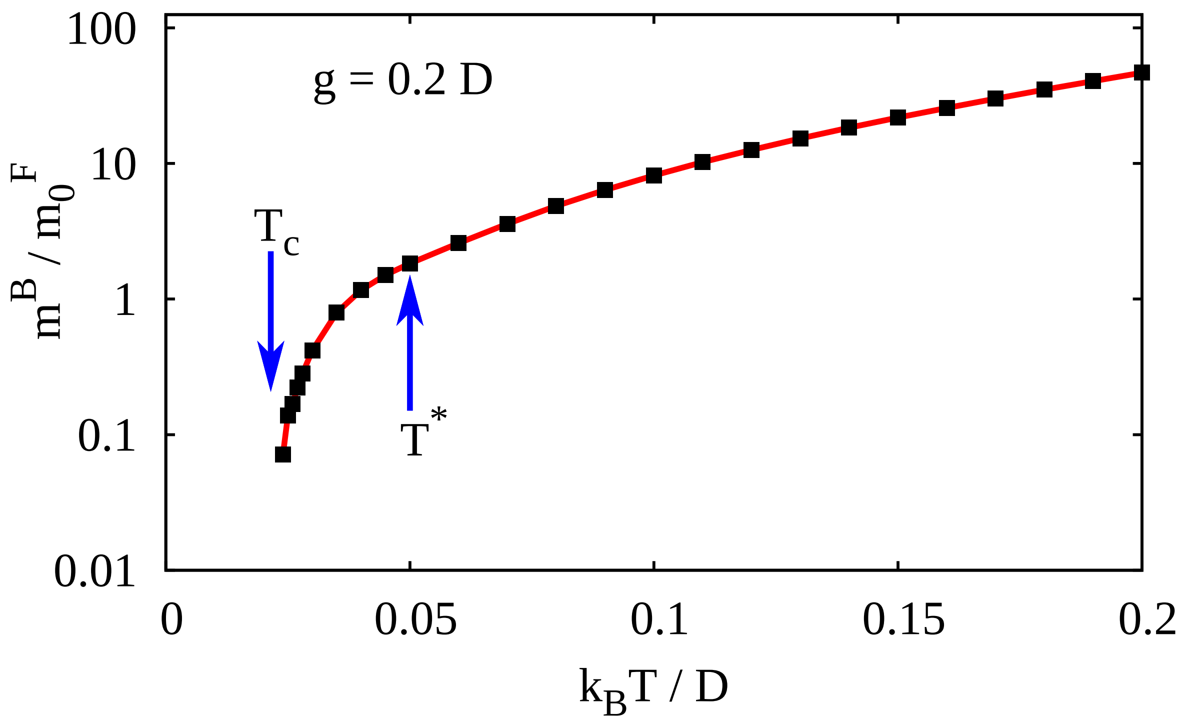

Effective mass m_B of the preformed pairs

M. Zapalska and T. Domański, Phys. Rev. B ***84****, 174520 (2011).*

Onset of diamagnetism above T_c

Onset of the diamagnetism is driven by the low-momentum preformed pairs.

T. Domański et al *(2016) submitted.*

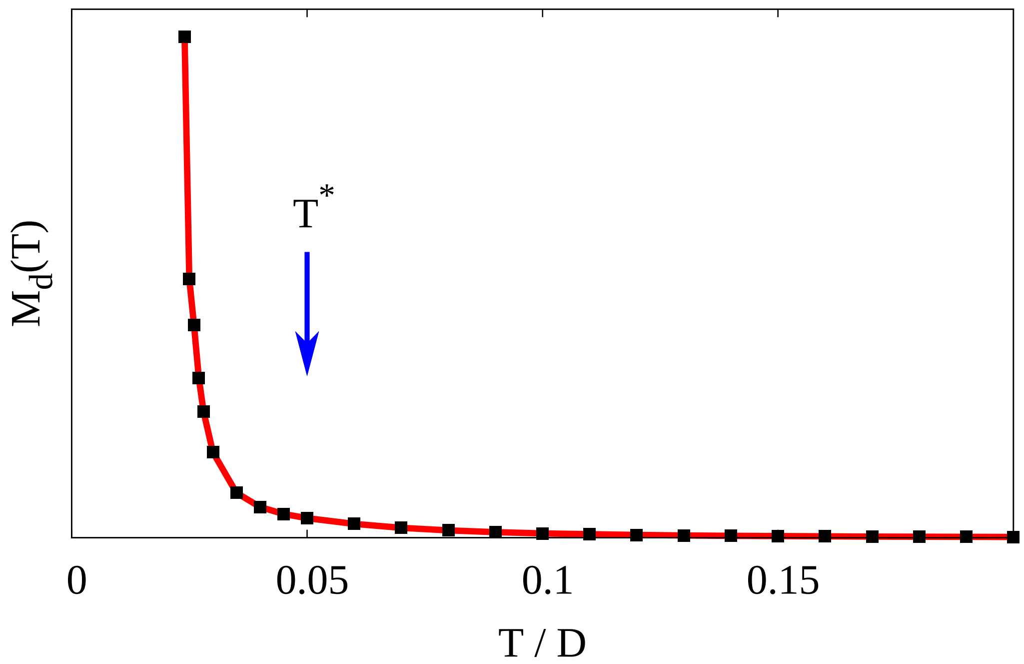

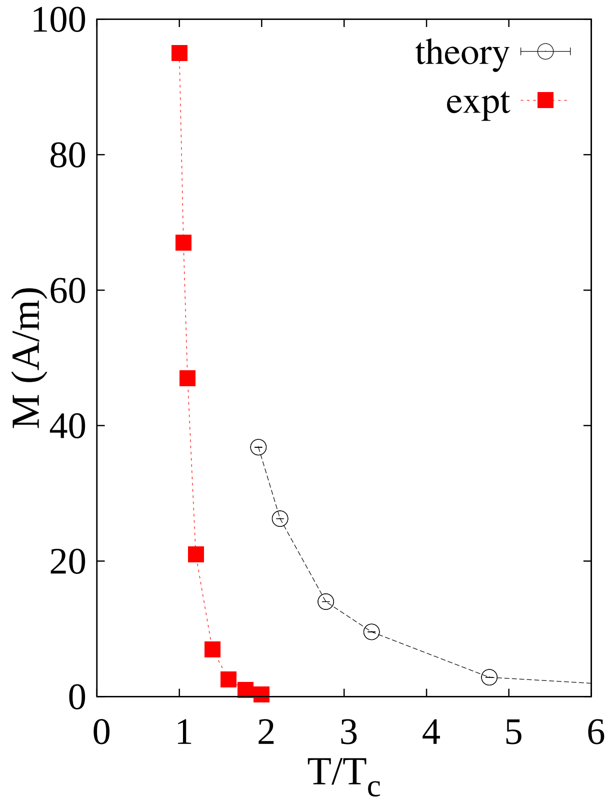

K.-Y. Yang, ... and M. Troyer, Phys. Rev. B **83**, *214516 (2011).*

Onset of diamagnetism above T_c

Onset of the diamagnetism is driven by the low-momentum preformed pairs.

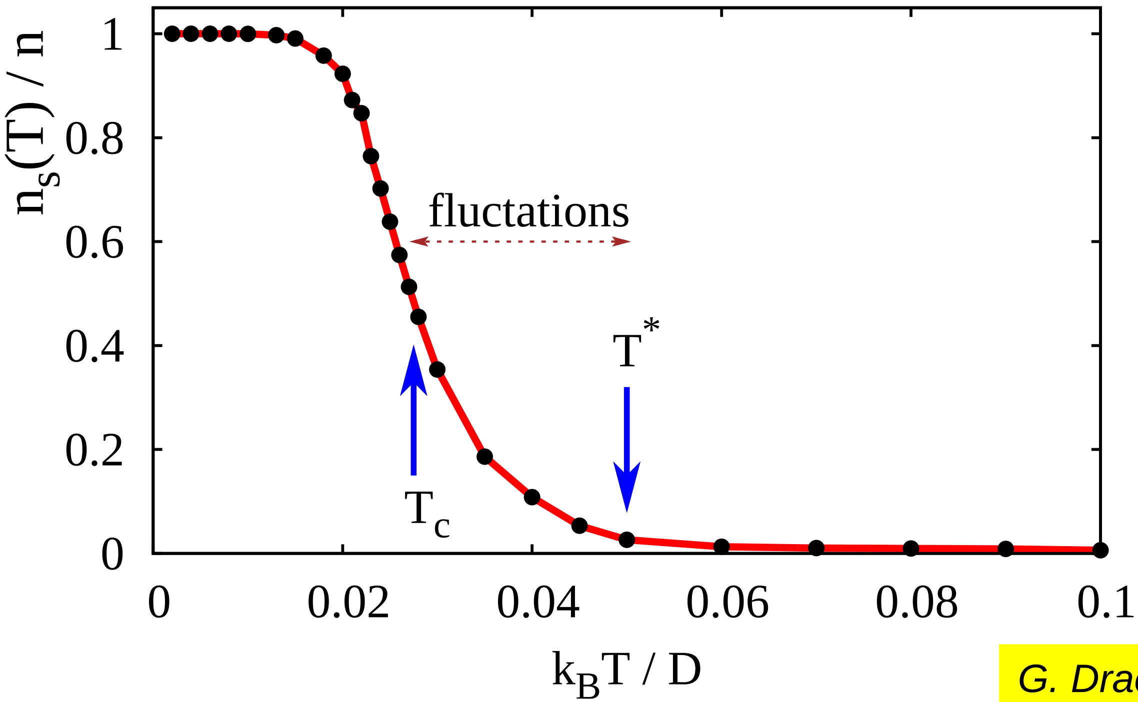

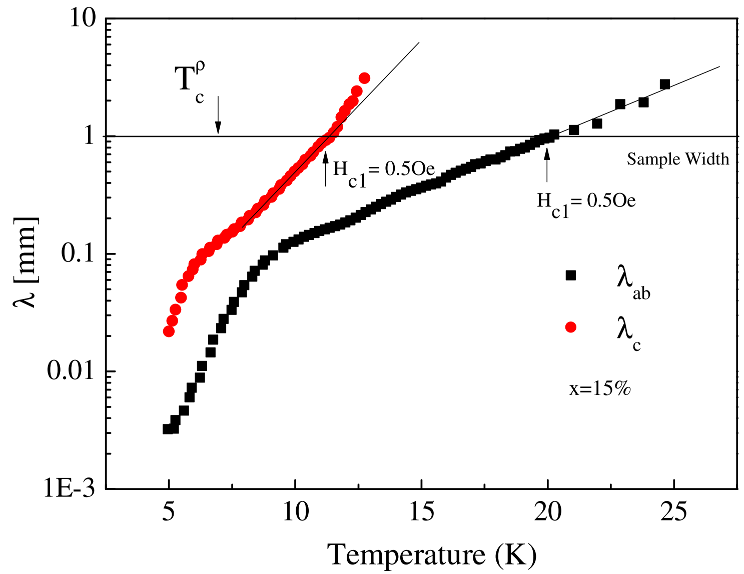

G. Drachuck et al, *Phys. Rev. B* **85**, *184518 (2012).*

$$J_x(\mathrm{q} \to 0, 0) = -\frac{e^2 n_s(T)}{m} A_x(\mathrm{q} \to 0, 0)$$

M. Zapalska and T. Domański, Phys. Rev. B **84**, *174520 (2011).*

Dynamic conductivity above T_c

Dynamic conductivity above T_c

Distribution of the low-momentum preformed pairs

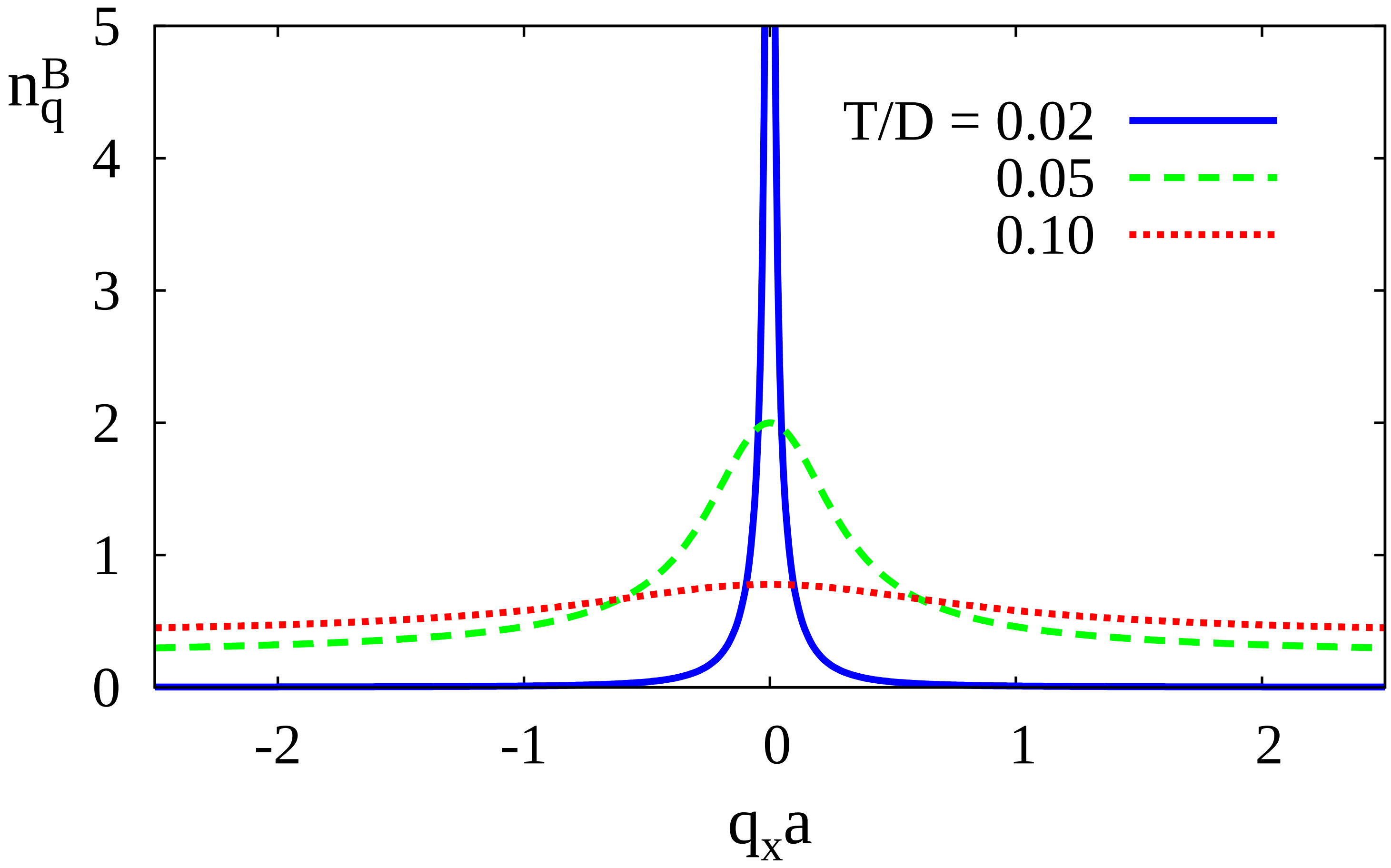

Dynamic conductivity above T_c

T. Domański et al *(2016) submitted.*

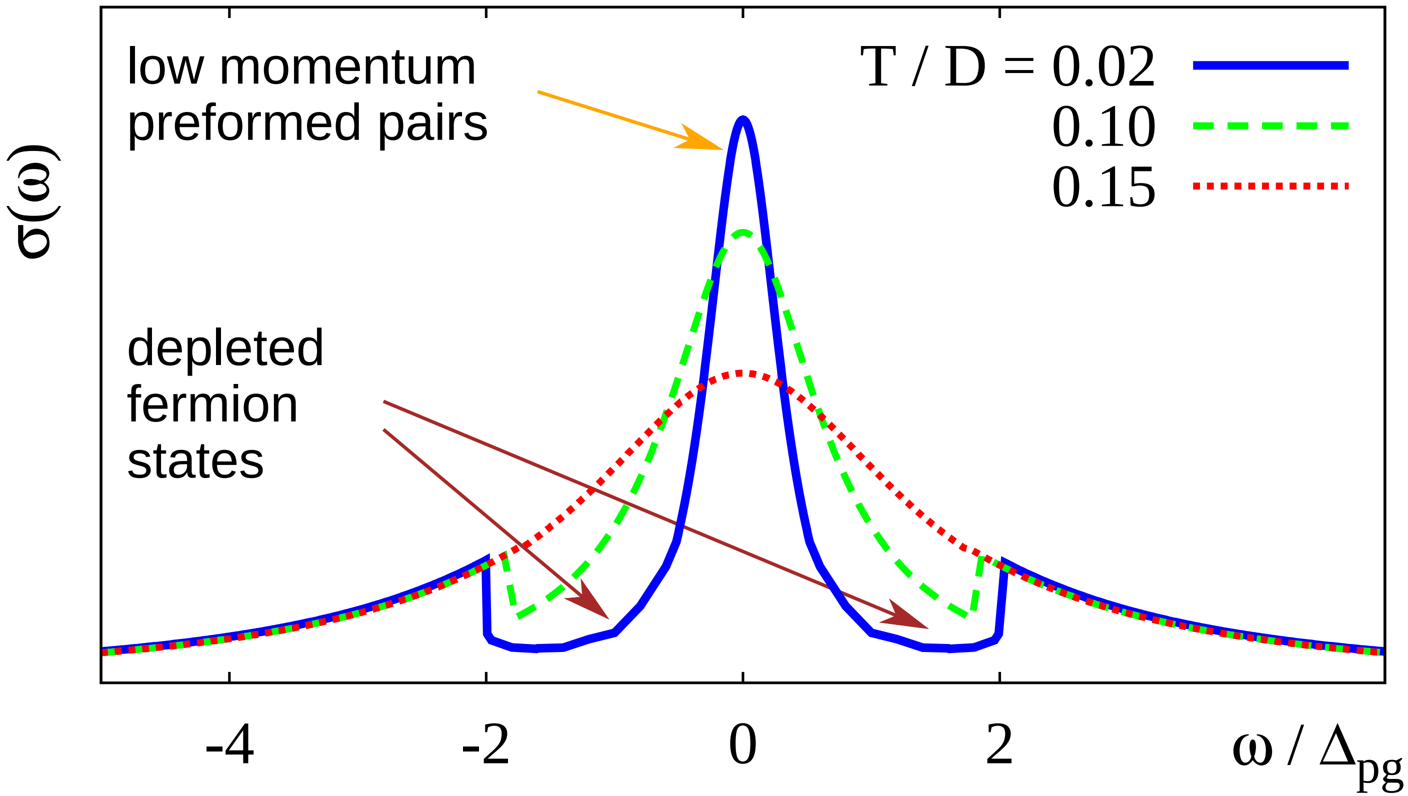

Qualitative effects: **optical gap + Drude peak**

caused by: **gaped spectrum + accumulation of low-momentum bosons**

Dynamic conductivity above T_c

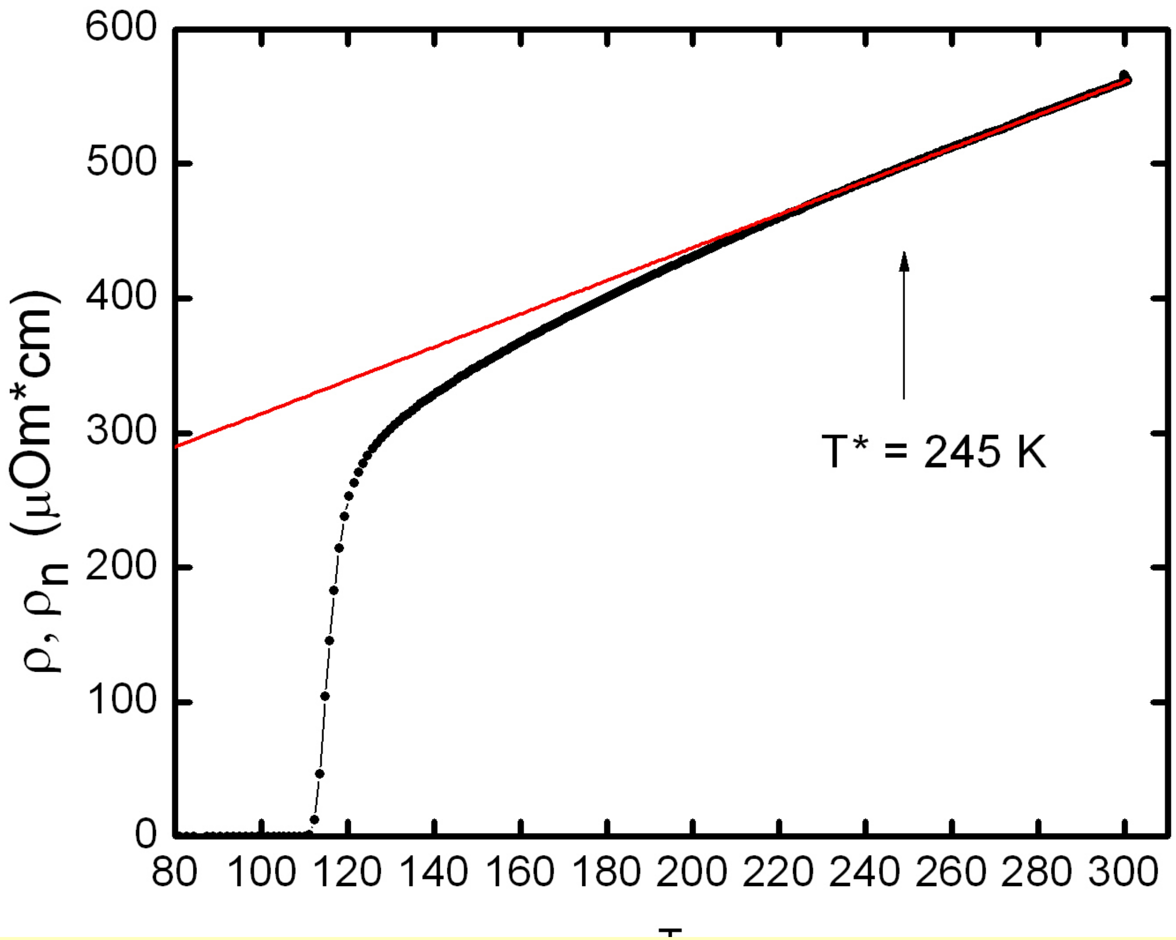

The d.c. resistivity of Bi2223 cuprate superconductors.

The fluctuation conductivity appears already at $T^* \approx 2.2 T_c$.

Dynamic conductivity above T_c

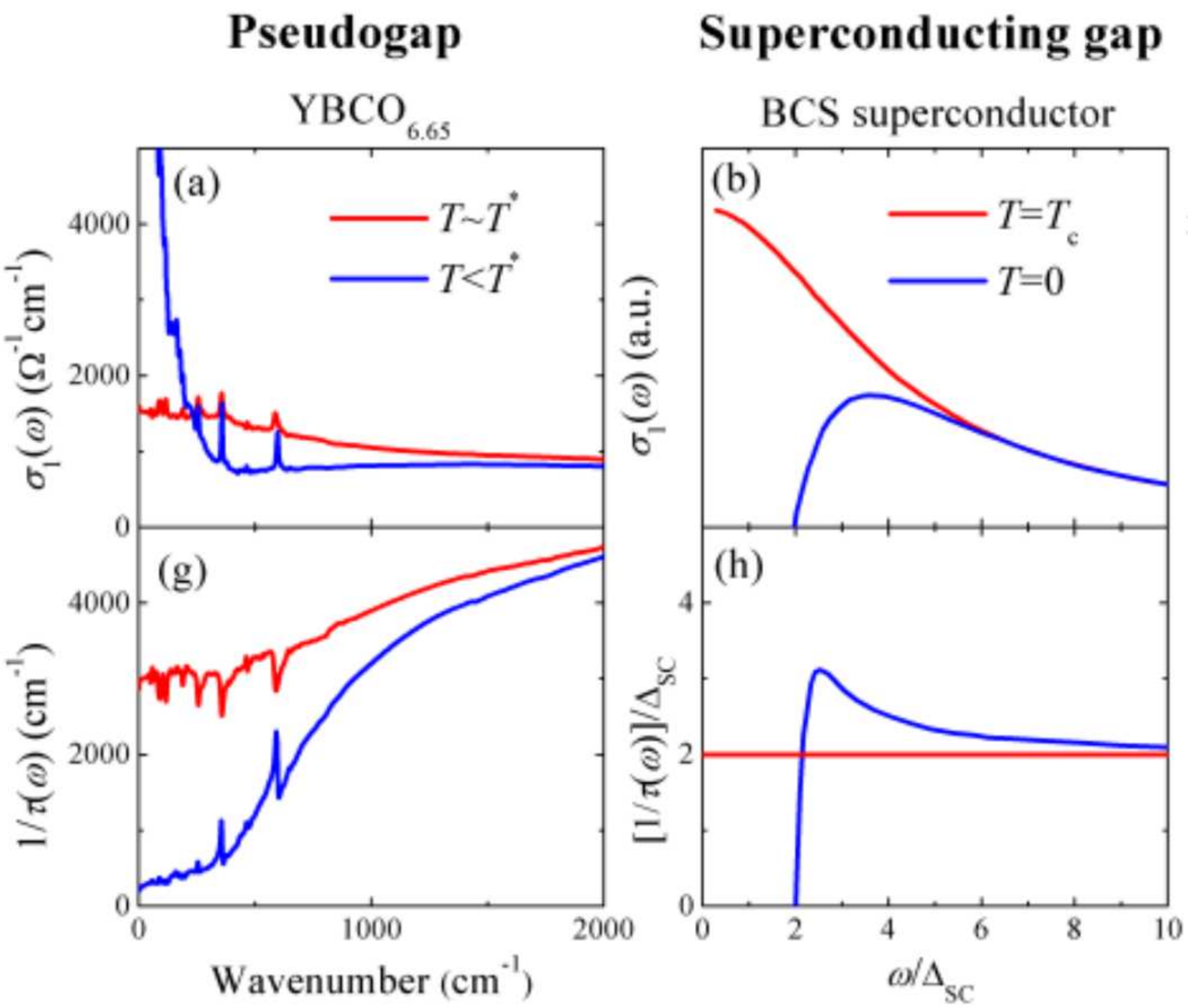

S.J. Moon et al, *Phys. Rev. B* **90**, *014503 (2014).*

Summary

Summary

- Experimental evidence for the pre-existing pairs above T_c

Summary

- **Experimental evidence for the pre-existing pairs above T_c**

$\Rightarrow$ **residual diamagnetism**

/ torque magnetometry, magnetization of needle samples /

Summary

- **Experimental evidence for the pre-existing pairs above T_c**

$\Rightarrow$ **residual diamagnetism**

/ torque magnetometry, magnetization of needle samples /

$\Rightarrow$ **fluctuation conductivity**

/ enhanced d.c. conductivity, Drude peak in a.c. conductivity/

Summary

- **Experimental evidence for the pre-existing pairs above T_c**

$\Rightarrow$ **residual diamagnetism**

/ torque magnetometry, magnetization of needle samples /

$\Rightarrow$ **fluctuation conductivity**

/ enhanced d.c. conductivity, Drude peak in a.c. conductivity/

$\Rightarrow$ **Bogoliubov quasiparticles**

/ ARPES, Josephson effect, FT-STM /

Summary

- **Experimental evidence for the pre-existing pairs above T_c**

$\Rightarrow$ **residual diamagnetism**

/ torque magnetometry, magnetization of needle samples /

$\Rightarrow$ **fluctuation conductivity**

/ enhanced d.c. conductivity, Drude peak in a.c. conductivity/

$\Rightarrow$ **Bogoliubov quasiparticles**

/ ARPES, Josephson effect, FT-STM /

- **These superconducting-like features are due to:**

Summary

- **Experimental evidence for the pre-existing pairs above T_c**

$\Rightarrow$ **residual diamagnetism**

/ torque magnetometry, magnetization of needle samples /

$\Rightarrow$ **fluctuation conductivity**

/ enhanced d.c. conductivity, Drude peak in a.c. conductivity/

$\Rightarrow$ **Bogoliubov quasiparticles**

/ ARPES, Josephson effect, FT-STM /

- **These superconducting-like features are due to:**

$\Rightarrow$ **the short-range correlations between the pairs**